FINITE ELEMENT ASSESSMENT OF PRECAST CONCRETE SLAB USING ANSYS STRUCTURAL

AMANKRAH KOJO ASARE

Department of NUCLEAR ENGINEERING

SCHOOL OF NUCLEAR AND ALLIED SCIENCES

COLLEGE OF BASIC AND APPLIED SCIENCES

UNIVERSITY OF GHANA

MPhil

JULY 2015

FINITE ELEMENT ASSESSMENT OF PRECAST CONCRETE SLAB USING ANSYS STRUCTURAL

A thesis submitted to the:

Department of NUCLEAR ENGINEERING

SCHOOL OF NUCLEAR &ALLIED SCIENCES

UNIVERSITY OF GHANA

By

AMANKRAH KOJO ASARE; 10442674

In partial fulfilment of the requirements for the award of

MASTER OF PHILOSOPHY DEGREE

IN

NUCLEAR ENGINEERING

JULY 2015

DECLARATION

I hereby declare that with the exception of references to other people's work which have been duly acknowledged, this compilation is the result of my own research work and no part of it has been presented for another degree in this University or elsewhere.

…… **Date**…….

AMANKRAH KOJO ASARE

(Candidate)

I hereby declare that the preparation of this project was supervised in accordance with the guidelines of the supervision of Thesis work laid down by University of Ghana.

…… ……

Dr. NII K. ALLOTEY **Dr. K. A. DANSO**

(PRINCIPAL SUPERVISOR) (Co-SUPERVISOR)

Date…… Date……

ABSTRACT

Concrete is used widely in all types of construction. In particular, it is the first choice material for the construction of various industries, due to its affordability, durability, heat resistance, strength, etc. Based on this, understanding the response of concrete structural components for all types of loading is crucial to the development of an overall safe and efficient structure.

Various methods have been used to study the response of concrete structural components to various loading regimes. Experimental based testing has been widely used as a means to analyse individual components; this method is, however, extremely time consuming and can be quite costly. Presently, the use of finite element analysis has increased due to increasing knowledge and capabilities of computer software and hardware. It has now become the best method to analyse concrete structural components.

In this study, a locally available precast concrete slab, termed the Trasaaco Fast Floor System, that is both reinforced and pre-stressed is analysed for its nonlinear behaviour under external imposed vertical loading conditions using the finite element (FE) method. The FE commercial software ANSYS 13.0, is used for the analysis.

Load-deflection responses and the crack patterns at critical stages of loading are studied. The results from the ANSYS programme are compared with technical data obtained from the Trasacco Group. The comparison shows the ANSYS programme to satisfactorily predict the behavioural responses of the fast floor slab system up to failure. In addition, the results obtained confirm the fact that Trasaaco Fast Floor System can be

potentially used to support the required loading regime for heavy industrial structures, like nuclear power plant facilities.

ACKNOWLEDGEMENTS

This research was accomplished under the guidance of Dr. Nii K. Allotey. I am really thankful for the guidance, knowledge, understanding, and numerous hours spent helping me complete this thesis. Gratitude is also extended to Dr. K. A Danso and Dr. E. Ampomah, for their time and efforts.

I would like to thank my parents, Paul and Patience Amankrah, and my siblings. Without my family, these accomplishments would not have been possible.

TABLE OF CONTENTS

LIST OF FIGURES

LIST OF TABLES

LIST OF SYMBOLS

Roman upper case letters

Ex	Modulus of elasticity
E_{ci}	Mean modulus of elasticity for concrete
E_{cm}	Secant modulus of elasticity of concrete

Roman lower case letters

e_{pA}	Load imbalance
f_{cb}	Biaxial compressive strength
f_{cm}	Mean compression strength of concrete
f_{cu}	Uniaxial compressive strength
f_{ps}	Characteristics tensile strength of prestressing steel
f_{yk}	Characteristics yield strength of reinforcement
f_z	Uniaxial tension strength
k_i	Stiffness
l	Length; span
u	Displacement

Greek letters

ε_c	Compressive strain in the concrete
ε_{c1}	Compressive strain in the concrete at the peak stress
ε_{uk}	Characteristic strain of reinforcement at maximum load

ε_{ps}	Strain of prestressing steel
σ_c	Compressive stress in the concrete
v	Poisson ratio

LIST OF ABBREVIATIONS

ANSYS	ANalysis SYStem
ASCE	America Society of Civil Engineers
ATENA	Advanced Tool for Engineering Nonlinear Analysis
CFRP	Carbon Fibre Reinforced Polymer
DOFs	Degrees of freedom
FE	Finite Element
GFRP	Glass Fibre Reinforced Polymer
GUI	Graphical user interface
IPCP	Ital Prestressed concrete products
N-R	Newton Raphson
PCG	Pre-condition CG
RC	Reinforced Concrete

CHAPTER 1

INTRODUCTION

1.1 General

Concrete is the world's most used man-made construction material today. It is fairly cheap and easy to form when cast. When concrete is cast, the cement locks the aggregate together making the concrete strong in compression. However, this lock mechanism does not help the concrete much in tension, and it is therefore weak in tension. To increase the tension capacity of the concrete and avoid cracks, it is *reinforced* with steel bars. Normal steel reinforcement, termed reinforced concrete (RC) does not always satisfactorily meet the required structural demands, pre-stressing in these cases is therefore required.

The concept of pre-stressing was introduced to generate compressive stresses in concrete prior to loading, by means of pre-stressing tendons inserted in the member. These compressive stresses work to resist the imposed tensile stresses, thereby efficiently increasing the cracking strength of the concrete member.

Slabs are plane structural members whose thickness is small in comparison with their long and short spans. Slabs are mostly used for floors, roof covering, and bridge decks. Slabs may be supported by walls or beams or directly by columns. It usually carries uniformly distributed gravity loads acting normal to their spans.

Concrete structural components behave differently under different variety of loading regimes. The identification and calculation of these responses is tiring and requires lot of expense and time. Currently there are numerous methods available to solve this

problem, among those methods, the one commonly used is the *FINITE ELEMENT (FE) METHOD*.

The Finite element method is a numerical analysis technique that divides the structural element into smaller elements, with each element providing a stiffness/load contribution to the global response of the structural element under the stated imposed loading condition. The method is very well-suited for nonlinear analyses as each component of the pre-stressed concrete member possesses different stress-strain properties. The FE tool frees designer's from the need to ponder on extensive mathematical calculations and allow them to spend more time on the accurate representation of the intended structure, and also a review of the calculated response.

Also, by using FE software (e.g., ANSYS, ATENA, etc.) with interactive graphical facilities, finite element models of complex structures can be created with ease, and obtain results in a convenient, readily assimilated form, that saves valuable design time.

1.2 Research problem statement

Most traditional building structures in developing countries rely on the conventional monolithic concrete slab-beam-column kind of construction. In these systems, the steel reinforcement placing and concrete casting for the different structural elements are done on site. This generally requires longer construction periods, as such, newer approaches including the use of precast concrete slab systems have gained ground in various developing countries, including Ghana.

With recent modularization of nuclear plants, the use of precast concrete systems is on the rise. However, a number of these system have not been studied in detail to ascertain their load carrying characteristics.

This thesis seeks to assess the response characteristics of a typical system in Ghana called the Trasacco Fast Floor System. It is currently widely used in the Ghanaian industry as the floor system for the floors of residential and commercial buildings. The thesis would thus seek to use the FE method to study the deformation response of a typical slab panel under monotonic vertical loading. This would enable an assessment to be made as to its competency as a potential slab system for heavy industrial plants like nuclear power plants.

1.3 Trasacco Fast Floor system

Trasacco Group, established in 1974, is made up of 12 separate companies. Ital pre-stress concrete products (IPCP) is one of the 12 companies. IPCP produces a range of pre-stress concrete products, including its leading brand, the Trasacco Fast Floor System.

Trasacco Fast Floors use pre-stressed concrete joists and hollow block system to produce floor and decking concrete slabs which can be used in the construction of commercial and residential buildings. This system has been a quick, robust and economical alternative to the existing and traditional buildings systems available in Ghana. Figure 1.1 shows the Trasacco Fast Floor setup.

Figure 1.1 Trasacco Fast Floors

1.4 Objectives and aims

The aim of this study is to understand the behaviour of a precast concrete slab system under various loading conditions. The main focus of the study will be on the nonlinear response of the precast concrete slab using finite element modelling.

The three arching objectives of the study are:

1. To create a finite element model of the precast concrete slab using ANSYS Version 13.0, and compare results of this model under monotonic vertical loading with the technical data obtained from the Trasacco Group (Trasacco, 2005).
2. To understand how the combined mechanism of the beam-slab system actually works under the imposed loading regime.
3. To assess whether the precast concrete slab system can be used in light and heavy industrial infrastructure, e.g., for nuclear power plant construction.

1.5 Outline of thesis

The thesis is divided into five chapters and is organized as per the detail given below:

Chapter 1: Provides a brief introduction on the topic.

Chapter 2: Provides a literature review on the topic, mainly focussing on work done by other researchers on the FE modelling of precast concrete slabs.

Chapter 3: Provides a discussion on FE modelling in relation to the ANSYS software.

Chapter 4: Provides a discussion on the results obtained.

Chapter 5: Presents conclusions and recommendations from the study.

CHAPTER 2

LITERATURE REVIEW

2.1 Introduction

A review of previous studies on the application of finite element method to the analysis of concrete structures is presented in this chapter, in addition to a discussion on the various loading regimes experienced by industrial structures. Additional material on the fundamental concept and use of the FE method to the analysis of linear and nonlinear concrete structures is accessible in the advanced reports by the American Society of Civil Engineers (ASCE, 1982) and Meyer and Okamura (1985).

2.2 Material

2.2.1 Concrete

Concrete is a composite material mixed mainly from cement, aggregate and water. Various materials can be added to the mixture to improve its properties like e.g. pozzolan, fly ash, sulphur, superplasticizer and fibers (Neville & Brooks, 2008). Concrete can therefore be made with different material properties regarding strength, durability and workability which make it popular as a construction material.

Concrete is a quasi-brittle material and behaves differently due to compression and tension. It is strong in compressions but has tensile strength usually only around 10% of its compression strength for normal concrete. Concrete, being ‘live’ material has some disadvantages. It creeps and shrinks which causes cracking.

The stress-strain relation for concrete, in compression, is in reality never fully linear and concrete is not an isotropic material. The stress-strain curve is, however, close to being linear up to 30%--40% of ultimate strength and estimation of the modulus of elasticity for concrete is usually based on that region of the curve.

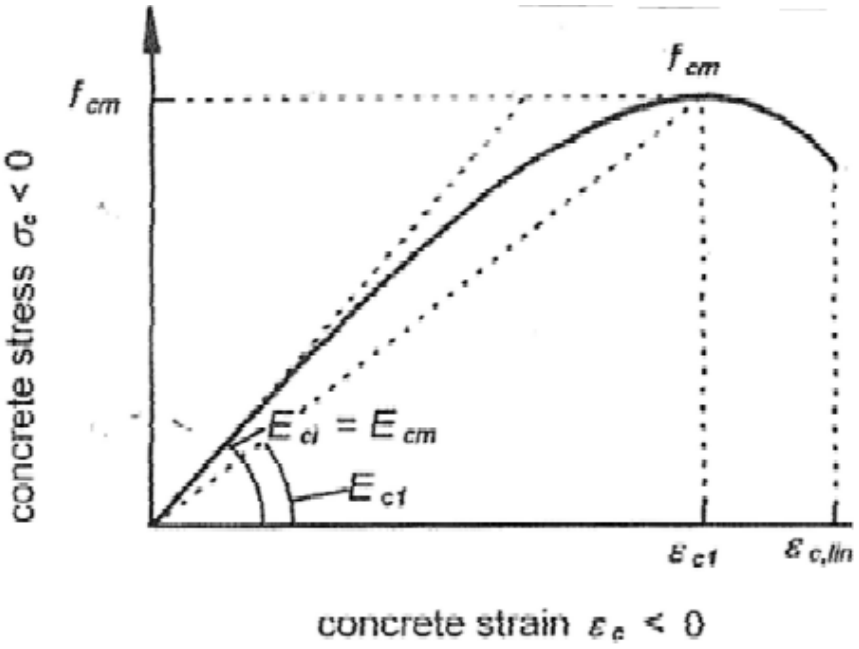

Figure 2.1: Stress-strain relation for uniaxial compression in concrete (Fib, 2012a).

When concrete reaches 70-80% of its ultimate strength, it starts to yield and exhibits plastic deformation. After the concrete has reached its ultimate strength, the stress-strain curve descends and crushing failure occurs at an ultimate strain (Kachlakev, 2001). Concrete therefore does not suffer from very brittle failure in compression except when pre-stressed.

2.2.2 Shear capacity of concrete

The behaviour of Reinforced concrete structures due to shear is a complex phenomenon and is still today partly unsolved. Few or no analytical methods are available

and calculations to estimate shear strength of reinforced concrete are mainly based on experimental equations developed from test results. However, it is known that shear resistance of reinforced concrete elements is mainly determined by contribution from aggregate interlock, dowel action, un-cracked compression zone and shear reinforcement. The nature of the interaction between concrete and reinforcement and mechanical properties of the reinforcing material have also some influence on the development of all of these shear mechanisms not just the concrete itself (Fib 2007).

2.2.3 Types of shear failure

When a concrete beam is loaded by a combination of shear force and bending moment, maximum shear and normal stresses at a point in a beam occur in planes inclined with the axis of the beam. These planes are usually called principal planes and the stresses that work on them are called principal stresses.

Above the neutral axis of the beam, the cross section of the beam is in compression and therefore the maximum principal stress is also in compression which prevents cracking. Below the neutral axis, where the beam cross section is in tension, the maximum principal stress is in tension. When the principal stress exceeds the concrete tensile strength, cracks form. The tension in the beam decreases as one moves toward the support and the slope of the principal stress rises. Because the concrete has relatively low tension strength, diagonal tension crack develops along planes perpendicular to the planes of principal tensile strength. Close to the supports where the cross section is almost in a state of pure shear, this diagonal tension forms inclined shear cracks (Nawy, 2009).

According to Nawy (2009), the effects of the tensile and flexural stresses are considerably reduced by pre-stressing concrete which leads to smaller flexural cracks in the pre-stressed member. This behaviour then directly affects the shear forces and the resulting principal stresses in the member, but those forces and stresses are considerably lower in a pre-stressed member than in an un-prestressed member.

Form of shear failure is different between members depending on several factors such as quantity of longitudinal reinforcement, geometry and load configuration. The shear span/effective depth ratio is one of the most significant factors affecting the behaviour of shear failure because it controls the slenderness of the member. Nawy (2009) stated that '*fundamentally, three modes of failure or their combination occur: flexural failure, diagonal tension failure, and shear compression failure'*.

When beams suffer from flexural failure, cracks start to develop in the middle of the beam perpendicular to the lines of principal stress. These cracks are therefore generally vertical and they extend towards the neutral axis as the load increases, causing noticeable deflection and finally failure of either the concrete or longitudinal reinforcement (Nawy, 2009).

Diagonal tension failure occurs when the diagonal tension strength is lower than flexural strength of the beam. First, vertical flexural cracks starts to develop at midspan which is followed by bonding failure between the reinforcing steel and surrounding concrete at the support. In continuation of that, diagonal cracks start to develop between loading and support points. As the cracks stabilize, they widen into principal diagonal tension cracks which extend to the top of the beam. This type of failure usually causes only relatively small deflection at failure.

Shear compression failure mode behaves similar to diagonal tension failure to begin with. That is, flexural cracks start to develop at midspan which is followed by bonding failure between the reinforcing steel and surrounding concrete close to the support. Next, inclined cracks quickly develop and head to the neutral axis; these cracks are, however, steeper than the cracks which developed in the diagonal tension failure. As the cracks get closer to the neutral axis, their progress slows down because concrete in the top compression fibers starts to crush and redistribute stresses in the compression zone. Finally the principal inclined cracks dynamically join the crushed concrete which causes sudden failure (Nawy, 2009).

2.2.4 Steel

Steel has been the most frequently used reinforcement material for concrete for a long time. Steel is used in various forms as reinforcement e.g. in form of high steel quality tendons which are usually stressed, in form of small fibers which are added to the concrete mixture before casting and in form of ordinary rebar's.

Steel is an isotropic material. Its main structural advantages are viscosity, stiffness and high strength. Its disadvantages include high density and corrosion. The stress-strain relation for normal and high strength reinforcement steel is reasonably linear up to the yield point but when the curve moves to plastic behaviour, it becomes nonlinear. The steel curve for normal steel behaves similar to concrete, that is, after it reaches ultimate stress, it starts decreasing as the strain increases and the failure is more ductile. The curve for high strength steel however fails when it reaches ultimate stress which results in more brittle failure than for normal steel.

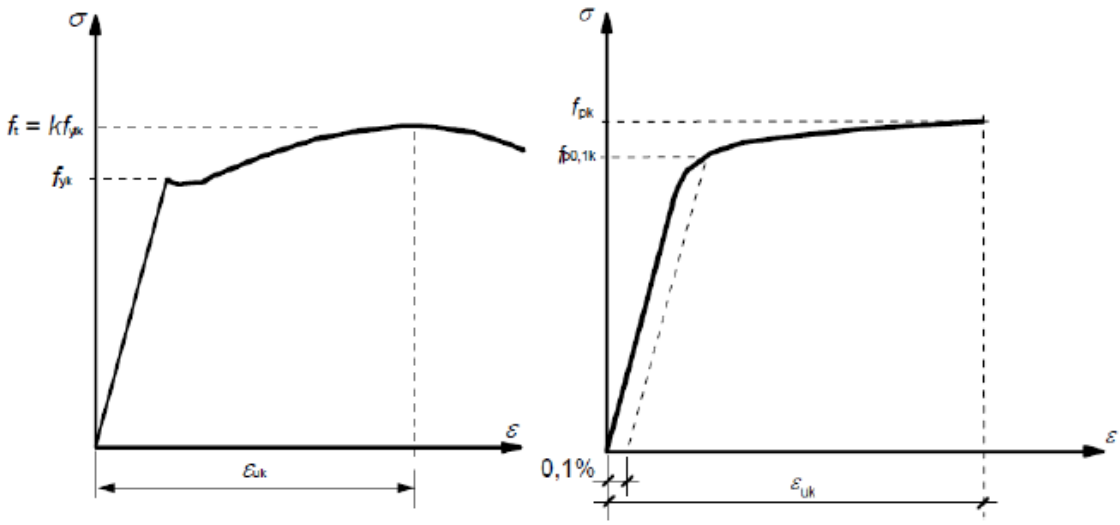

Figure 2.2: Stress-strain relation for hot rolled normal steel reinforcement (Left). Stress-strain relation for typical high strength steel (Right). (BS EC2, 2004)

2.3 FE analysis of precast concrete structures

Two different methods have been used so far for the analysis of reinforced concrete slabs by the FE method: the modified stiffness approach and the layer approach. The former is based on an average moment-curvature relationship which reflects the various stages of material behaviour, while the latter subdivides the finite element into imaginary concrete and steel layers with idealized stress-strain relations for concrete and reinforcing steel.

Dotroppe et al. (1973) used a layered finite element procedure in which slab elements were divided into layers to account for the progressive cracking through the slab thickness. Scanlon and Murray (1974) have developed a method of incorporating both cracking and time-dependent effects of creep and shrinkage in slabs. They used layered rectangular slab elements which could be cracked progressively layer by layer, and assumed that cracks propagate only parallel and perpendicular to orthogonal reinforcement.

In one of the pioneering early studies, Rashid (1968) introduced the concept of a "smeared" crack in the study of the axisymmetric response of pre-stressed concrete reactor structures. Rashid took into account cracking and the effects of temperature, creep and load history in his analyses. Today the smeared crack approach of modelling the cracking behaviour of concrete is almost exclusively used by investigators in the nonlinear analysis of RC structures, since its implementation in a finite element analysis program is simpler than that of the discrete crack model. Computer time considerations also favour the smeared crack model in analyses which are concerned with the global response of structures. At the same time, the concerted effort of many investigators in the last 20 years has removed many of the limitations of the smeared crack model (ASCE 1982; Meyer and Okamura, eds. 1985).

Gilbert and Warner (1978) used the smeared crack model and examined the effect of the slope of the descending branch of the concrete stress-strain relation on the behaviour of reinforced concrete (RC) slabs. They were among the first to point out that analytical results of the response of reinforced concrete structures are greatly influenced by the size of the finite element mesh and by the amount of tension stiffening of concrete. Several studies followed which corroborated these findings and showed the effect of mesh size (Bazant and Cedolin 1980; Bazant and Oh 1983; Kwak 1990) and tension stiffening (Barzegar and Schnobrich 1986; Leibengood et al. 1986) on the accuracy of finite element analyses of RC structures with the smeared crack model.

2.4 Modelling with ANSYS software

Barbosa and Ribeiro (1998) examined the possibilities of performing nonlinear finite element analysis of reinforced concrete structures using ANSYS concrete model. In

this study, nonlinear stress-strain relations for concrete in compression were made to reach the ultimate load so as to determine the entire load–deflection diagram. The results suggested the satisfactory prediction of the response of reinforced concrete structure could be obtained with the ANSYS programme.

Zhang and Hussein (2004) presented the application of the FE method for the numerical modelling of punching shear failure mode using ANSYS. The authors studied the behaviour of slab-column connections reinforced with Glass Fibre Reinforced Polymers. (GFRP). SOLID65 and LINK8 elements represented concrete and reinforcing steel bars, respectively. A spring element LINK10, along the edge, was included in this study to reflect the actual set up of slab-column connection. A quarter of the full size slab-column connections, with appropriate boundary conditions, were used in ANSYS for modelling. Concrete constitutive relationships included the elastic–perfectly plastic model, crack condition and crush limit. The GFRP reinforcement was defined as linear elastic. Spring supports were compression only elements. The author stated that general behaviour of the finite element model represented by the load-deflection plots at the centre showed good agreement with the test data. However, the finite element models showed slightly more stiffness than the test data in both linear and nonlinear ranges.

Kachlakev, et al. (2001) used ANSYS to study concrete beam members with externally bonded Carbon Fibre Reinforced Polymer (CFRP) fabric. Symmetry allowed one quarter of the beam to be modelled. At planes of symmetry, the displacement in the direction perpendicular to the plane was set to zero. A single line support was used to allow rotation at the supports. Loads were placed at third points along the full beam on top of

steel plates. The mesh was refined immediately beneath the load. No stirrup-type reinforcement was used.

The nonlinear Newton-Raphson approach was used to trace the equilibrium path during the load-deformation response. It was discovered that convergence of solutions for the model was difficult to achieve due to the nonlinear behaviour of reinforced concrete material. At selected stages in the analysis, load step sizes were varied from large (at points of linearity in the response) to small (when instances of cracking and steel yielding occurred). The load-deflection curve for the non-CFRP reinforced beam was plotted and showed reasonable correlation with experimental data (McCurry and Kachlakev 2000).

It is noted from the study that for concrete beam elements, failure modes that can occur are: flexural cracks, compression failure (crushing), and diagonal tension cracks. Flexural cracks form vertically up the beam. Compression failures form as circles. Diagonal tension cracks form diagonally up the beam towards the loading that is applied. The study further indicates that the use of a FE program to model experimental data is viable, and that the results obtained can indeed model reinforced concrete beam behaviour reasonably well.

2.5 Failure surface models for concrete

William and Warnke (1974) developed a widely used model for the triaxial failure surface of unconfined plain concrete. The failure surface in principal stress-space is shown in Figure 2.3. The mathematical model considers a sextant of the principal stress space because the stress components are ordered according to $\sigma_1 \geq \sigma_2 \geq \sigma_3$ .These stress components are the major principal stresses.

The failure surface is separated into hydrostatic (change in volume) and deviatoric (change in shape) sections as shown in Figure 2.4. The hydrostatic section forms a meridianal plane which contains the equisectrix $\sigma_1 = \sigma_2 = \sigma_3$ as an axis of revolution (see Figure 2.3). The deviatoric section in Figure 2.4 lies in a plane normal to the equisectrix (dashed line in Figure 2.4).

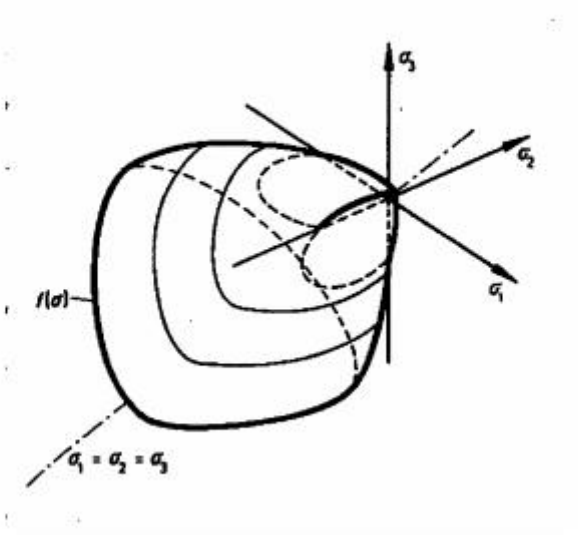

Figure 2.3 – Failure Surface of Plain Concrete under Triaxial Conditions

(Willam and Warnke 1974)

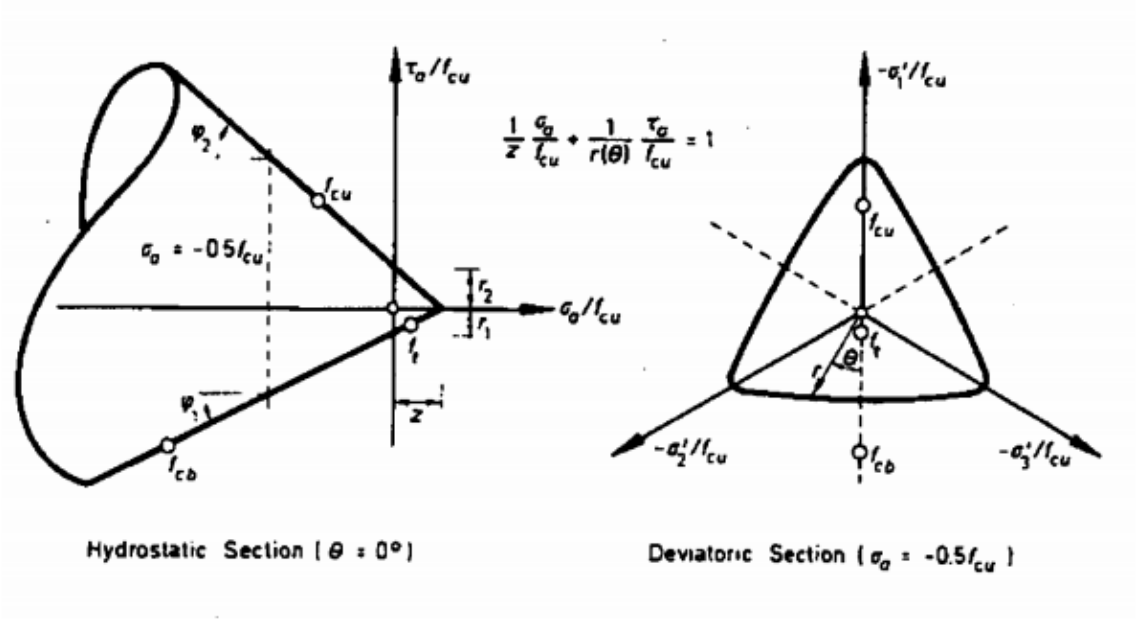

Figure 2.4 – Three Parameter Model (Willam and Warnke 1974)

The deviatoric trace is described by the polar coordinates ***r, and θ*** where *r* is the position vector locating the failure surface with angle, ***θ***. The failure surface is defined as:

$$\frac{1}{z}\frac{\sigma_a}{f_{cu}} + \frac{1}{r(\theta)}\frac{\tau_a}{f_{cu}} = 1 \qquad (2.1)$$

Where:

σ_a and τ_a = average stress components

z = apex of the surface

f_{cu} = uniaxial compressive strength

The opening angles of the hydrostatic cone are defined by $\boldsymbol{\varphi_1}$ **and** $\boldsymbol{\varphi_2}$. The free parameters of the failure surface ***z and r***, are identified from the uniaxial compressive strength ($\boldsymbol{f_{cu}}$), biaxial compressive strength ($\boldsymbol{f_{cb}}$), and uniaxial tension strength ($\boldsymbol{f_z}$)

The Willam and Warnke (1974) mathematical model of the failure surface for the concrete has the following advantages:

1. Close fit of experimental data in the operating range;
2. Simple identification of model parameters from standard test data;
3. Smoothness (e.g. continuous surface with continuously varying tangent planes);
4. Convexity (e.g. monotonically curved surface without inflection points).

Based on the above criteria, a constitutive model for the concrete suitable for FE analysis implementation was formulated.

This constitutive model for concrete based upon the Willam and Warnke (1974) model assumes an appropriate description of the material failure. The yield condition can be approximated by three or five parameter models distinguishing linear from non-linear and elastic from inelastic deformations using the failure envelope defined by a scalar function of stress $\boldsymbol{f}(\boldsymbol{\sigma}) = \mathbf{0}$ through a flow rule, while using incremental stress-strain relations. The parameters for the failure surface can be seen in Figure 2.4.

During transition from elastic to plastic or elastic to brittle behaviour, two numerical strategies were recommended: proportional penetration, which subdivides proportional loading into an elastic and inelastic portion which governs the failure surface using integration, and normal penetration, which allows the elastic path to reach the yield surface at the intersection with the normal therefore solving a linear system of equations.

Both of these methods are feasible and give stress values that satisfy the constitutive constraint condition. From the standpoint of computer application the normal penetration

approach is more efficient than the proportional penetration method, since integration is avoided.

2.6 FE modelling of steel reinforcement

Tavarez (2001) discusses three techniques that exist to model steel reinforcement in finite element models for reinforced concrete (Figure 2.5); these are: the discrete model, the embedded model, and the smeared model.

The reinforcement in the discrete model (Figure 2.5a) uses bar or beam elements that are connected to concrete mesh nodes. Therefore, the concrete and the reinforcement mesh share the same nodes and concrete occupies the same regions occupied by the reinforcement. A downside to this model is that the concrete mesh is restricted by the location of the reinforcement and the volume of the steel reinforcement is not deducted from the concrete volume.

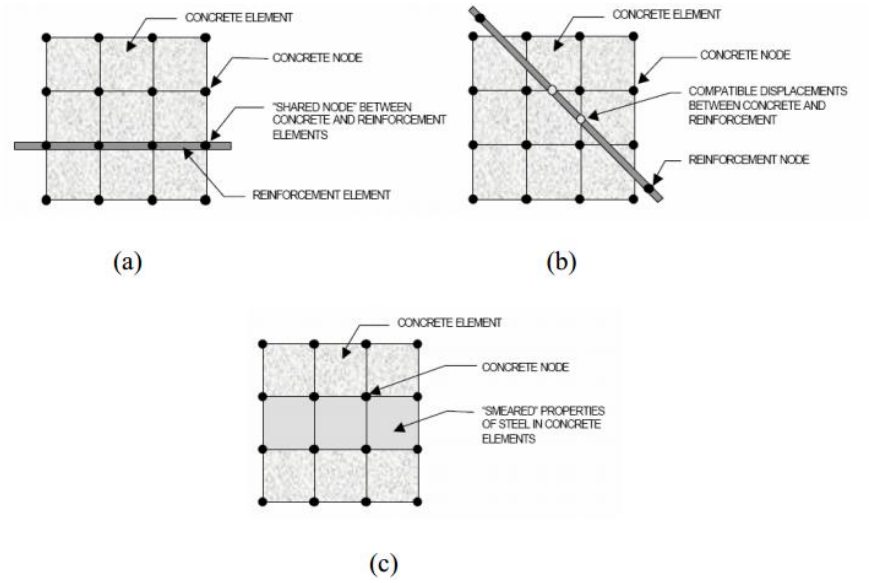

Figure 2.5 – Models for Reinforcement in Reinforced Concrete (Tavarez 2001): (a) Discrete; (b) embedded; and (c) smeared

The embedded model (Figure 2.5b) overcomes the concrete mesh restriction(s) because the stiffness of the reinforcing steel is evaluated separately from the concrete elements. The model is developed in a way that keeps reinforcing steel displacements compatible with the surrounding concrete elements. When reinforcement is complex, this model is very advantageous. However, this model increases the number of nodes and degrees of freedom in the model, therefore, increasing the run time and computational cost.

The smeared model (Figure 2.5c) assumes that reinforcement is uniformly spread throughout the concrete elements in a defined region of the FE mesh. This approach is used for large-scale models where the reinforcement does not significantly contribute to the overall response of the structure.

Fanning (2001) modelled the response of the reinforcement using the discrete model and the smeared model for reinforced concrete beams. It was found that the best modelling strategy was to use the discrete model when modelling reinforcement.

2.7 Remarks on ANSYS FE modelling of concrete

The literature review provided suggests that use of the ANSYS FE package to model reinforced and pre-stressed concrete is indeed feasible. It was decided to use ANSYS as the finite element modelling package for this thesis.

In summary, Bjarnason (2008) has noted that if the FE method is used in nonlinear analysis with appropriate constitutive relationships, failure and deformational characteristics, then realistic behaviour of pre-stressed concrete can be predicted.

2.8 Imposed loading regimes on industrial structures

The probable failure assessment of structures for heavy industrial facilities like nuclear power facilities has bearings on the choice and postulation of the loads and load combinations. Critical structures like nuclear power plant are designed for normal service dead and imposed load as well as extreme loads.

2.8.1 Service Loads

- Dead load: Dead loads consist of the weight of all materials of construction incorporated into the building including, but not limited to, walls, floors, roofs, ceilings, stairways, built-in partitions, finishes, cladding, and other similarly incorporated architectural and structural items, and fixed service equipment including the weight of cranes.

- Live loads: A load produced by the use and occupancy of the building or other structure that does not include construction or environmental loads, such as wind load, snow load, rain load, earthquake load, flood load, or dead load. The live loads used in the design of buildings and other structures is the maximum loads expected by the intended use or occupancy, but should not be less than the minimum uniformly distributed unit loads required.

Table 2.1 Minimum uniformly distributed live loads

Occupancy or use	Uniform distributed loads
Manufacturing	
Light	6.00 kN/m^2
Heavy	11.97 kN/m^2
Storage warehouse	
Light	6.00 kN/m^2
heavy	11.97 kN/m^2

2.8.2 Severe Loads

- Seismic Load: The severe seismic load is typically defined in National Building Codes as a general requirement for all buildings or other facilities with human occupancy. It is often defined as the equivalent to a median 2×10^{-3}/yr or 10 percent probability of exceedance in 50 years for ordinary buildings, and 1×10^{-3}/yr for essential or commercially hazardous buildings by use of a 1.25 importance multiplication factor applied to ordinary building equipment seismic loads (John D. Stevenson and Ovidiu Comam).
- Wind and Precipitation (Rain, Snow or Ice) Loads, W, S: The design basis wind velocity is also defined on a probabilistic basis. Its selection is typically based on either a several-minute average fastest wind or more recently, since 1995, on a maximum 3-second gust wind speed for a 50-year recurrence interval or 2×10–2 mean probability of exceedance for the site exposure level based on the ASCE-7 Standard (ASCE, 2005).

CHAPTER 3

FINITE ELEMENT MODELLING

3.1 FE method

This method is based on dividing problem domain into several small elements. These small elements are then analysed by applying known physical laws to each of them. The behaviour of each sub-domain, which is shaped by nodes and element, is then approached by using piecewise linear functions to represent continuous function of an unknown field variable. The unknown represents the discrete values of the field variable at the nodes. Then appropriate principles are used to develop equations for the elements which are then combined to one another. The result of this process is a set of linear algebraic simultaneous equations which represent the whole system. These equations can then be solved to return the necessary field variable (Liu and Qeck, 2003).

When creating a finite element model, an element type must first be chosen to define the geometry and degrees of freedom. There are numerous element type in ANSYS that can be used, e.g. link, beam, plate, 2D solid and shell elements. The main differences between these elements are due to amount of degrees of freedom as well as possibilities of shape and how they deform. According to Liu and Qeck, (2003), these elements can, however all be considered as special case of a three-dimensional (3D) solid element, which is considered the most general of all solid FE elements. In 3D solid elements, field variables depend on x, y and z directions. It can also have any arbitrary shape, boundary condition and material properties in space meaning it can deform in all three directions in space.

3.2 ANSYS Finite Element Model

To create the finite element model in ANSYS, multiple tasks need to be completed before the model can run properly. Models can be created using command prompt input or the Graphical User Interface (GUI). For this model, the GUI was used to create the model.

3.2.2 Element Types

The Solid65 element was used to model the concrete. This element has eight nodes with three degrees of freedom at each node – translations in the nodal x, y, and z directions. This element is capable of plastic deformation, cracking in three orthogonal directions, and crushing. A schematic of the element is shown in Figure 3.1.

Table 3.1: Element types

Material type	ANSYS element
Concrete	Solid65
Stirrups and top bar	Link180
Tendons	Link180

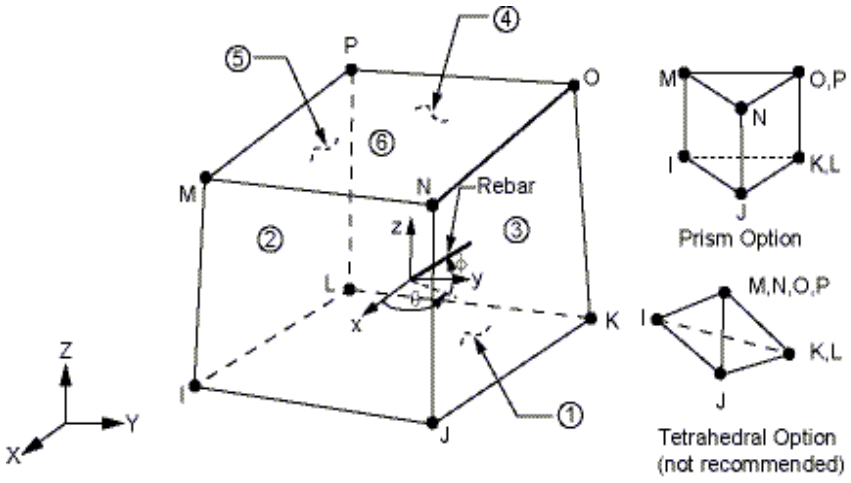

Figure 3.1: Solid65 Element (ANSYS, 2011)

The Link180 element was used to model the stirrups and tendons. This element is a 3D element and it has two nodes with three degrees of freedom – translations in the nodal x, y, and z directions. This element is also capable of plastic deformation. The element is shown in Figure 3.2.

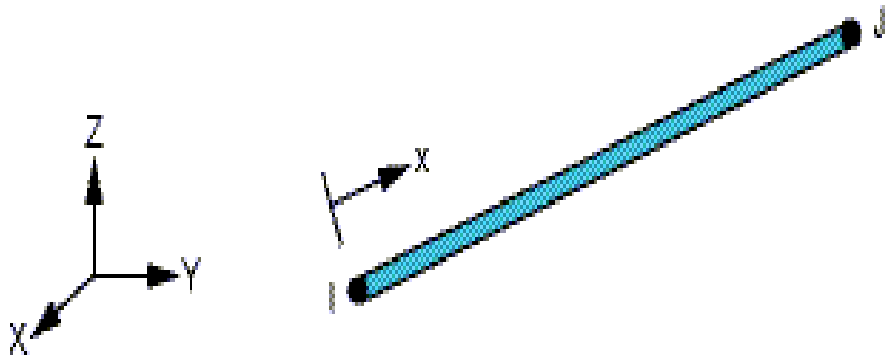

Figure 3.2: Link180 Element (ANSYS, 2011)

3.2.3 Real Constants

Real Constant Set 1 is used for the Solid65 element. It requires real constants for rebar assuming a smeared model. Values can be entered for Material Number, Volume Ratio, and Orientation Angles. The material number refers to the type of material for the reinforcement. The volume ratio refers to the ratio of steel to concrete in the element. The orientation angles refer to the orientation of the reinforcement in the smeared model. ANSYS allows the user to enter three rebar materials in the concrete. Each material corresponds to x, y, and z directions in the element (Figure 3.1). A value of zero was entered for all real constants which turned the smeared reinforcement capability of the Solid65 element off.

Table 3.2: Real constants

Real constant set	Element type		Constants		
			rebar 1	rebar 2	rebar 3
1	Solid65	Material number	0	0	0
		Volume ratio	0	0	0
		Orientation angle	0	0	0
		Orientation angle	0	0	0
2	Link180	cross-sectional area	47.72 mm^2		
3	Link180	cross-sectional area	113 mm^2		
4	Link180	cross-sectional area	502.5 mm^2		
5	Link180	cross-sectional area	402 mm^2		

The cross-sectional area for Real Constant Set 2 is the area of the 3-wire strand up to seven strands 3 x 2.25 of 11.93 mm^2. Real Constant Set 3 is the area of the 12 mm diameter rod bar which were used for the stirrups. Real Constant Sets 4 and 5 are the areas of the 16 mm diameter bar rods that are used for the longitudinal steel of the edge beams obtained from the representative slab-beam design drawing obtained from a local engineering consulting office in Accra that is based on the Trasacco floor system (Strescon, 2014).

3.2.4 Material Properties

The Solid65 element requires linear isotropic and multi-linear isotropic material properties to correctly model the concrete material. The multi-linear isotropic material uses

the von Mises failure criterion along with the Willam and Warnke (1974) model to define the failure of the concrete. The required linear inputs are the modulus of elasticity of the concrete (*Ex*), and Poisson's ratio (*v*). The compressive uniaxial stress-strain relationship for the concrete model was obtained using the equation from British Standard Eurocode 2 (BS EC2, 2004) to compute the multi-linear isotropic stress-strain curve for the concrete.

$$\frac{\sigma_c}{f_{cm}} = \frac{k\eta - \eta^2}{1+(k-2)\eta} \tag{3.1}$$

Where

$\eta = \frac{\varepsilon_c}{\varepsilon_{c1}}$

ε_{c1} = is the strain at peak stress.

$k = 1.05E_{cm} * \frac{\varepsilon_{c1}}{f_{cm}}$

f_{cm} = Mean value of concrete cylinder compressive strength

E_{cm} = Secant modulus of elasticity of concrete

The multi-linear isotropic stress-strain curve implemented requires the first point of the curve to be defined by the user. It must satisfy Hooke's law:

$$E = \frac{\sigma}{\varepsilon} \tag{3.2}$$

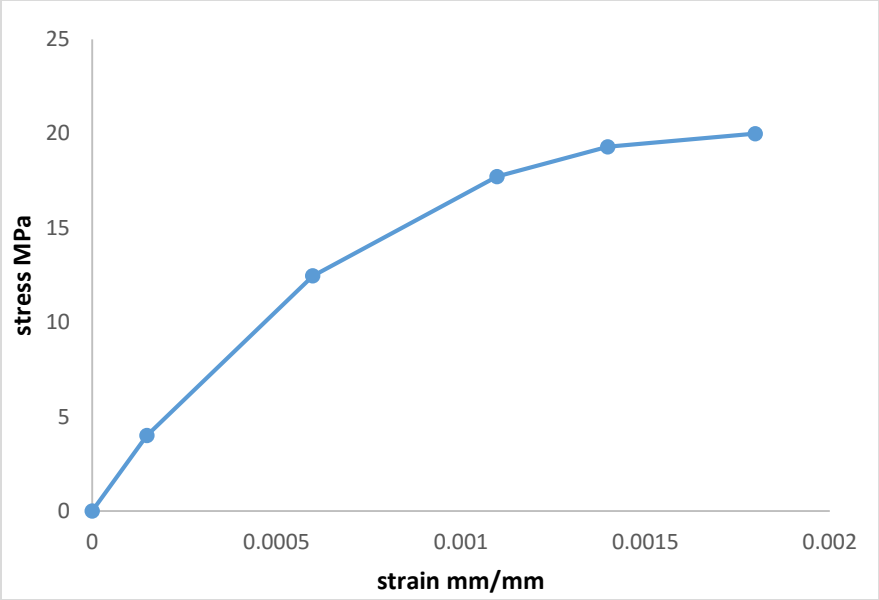

Figure 3.3: Uniaxial stress-strain curve for C12 concrete

The curve was constructed by marking six points and connecting them with straight lines. The curve starts at zero stress and strain. The first point was defined according to equation (3.2) with the stress being 20% of f_{cm}. Rests of the points were defined according to equation (3.1). The value of the compression strength for point 2, 3 and 4 were chosen with similar distribution as in the work of Kachlakev, et al. (2001).

- For point two, the stress was chosen as approximately 60% of f_{cm}.
- For point three, the stress was chosen as approximately 85% of f_{cm}.
- For point four, the stress was chosen as approximately 96% of f_{cm}.
- The fifth point is the peak stress

All calculations for the different grades of the concrete stress-strain curves are shown in Appendix A (please note that C12 means concrete with a cube compression strength of 12 MPa). The multi-linear curve is used to help with convergence of the nonlinear solution algorithm.

Implementation of the Willam and Warnke (1974) material model in ANSYS requires that different constants be defined. These 9 constants are:

1. Shear transfer coefficients for an open crack;
2. Shear transfer coefficients for a closed crack;
3. Uniaxial tensile cracking stress;
4. Uniaxial crushing stress (positive);
5. Biaxial crushing stress (positive);
6. Ambient hydrostatic stress state for use with constants 7 and 8;
7. Biaxial crushing stress (positive) under the ambient hydrostatic stress state (constant 6);
8. Uniaxial crushing stress (positive) under the ambient hydrostatic stress state (constant 6);
9. Stiffness multiplier for cracked tensile condition.

Typical shear transfer coefficients range from 0.0 to 1.0, with 0.0 representing a smooth crack (complete loss of shear transfer) and 1.0 representing a rough crack (no loss of shear transfer). The shear transfer coefficients for open and closed cracks were determined using the work of Kachlakev, et al. (2001) as a basis. Convergence problems occurred when the shear transfer coefficient for the open crack dropped below 0.2. No deviation of the response occurred with the change of the coefficient. Therefore, the coefficient for the open crack was set to 0.4. The uniaxial cracking and crushing stress was determined from the European Standards for Reinforced Concrete (BS EC2 (2004)).

The biaxial crushing stress refers to the ultimate biaxial compressive strength. The ambient hydrostatic stress state is denoted as σ_h. This stress state is defined as:

$$\sigma_h = \frac{1}{3}(\sigma_{xp} + \sigma_{yp} + \sigma_{zp}) \tag{3.3}$$

where $\sigma_{xp}, \sigma_{yp}\ and\ \sigma_{zp}$ are the principal stresses in the principal directions. The biaxial crushing stress under the ambient hydrostatic stress state refers to the ultimate compressive strength for a state of biaxial compression superimposed on the hydrostatic stress state (f_1). The uniaxial crushing stress under the ambient hydrostatic stress state refers to the ultimate compressive strength for a state of uniaxial compression superimposed on the hydrostatic stress state (f_1). The failure surface can be defined with a minimum of two constants, (f_t) and $(f_c{}')$. The remainder of the variables in the concrete model were left to the default ANSYS values.

The Link180 element was used to model all stirrups in the beam and tendons in the joist. The stress-strain behaviour is assumed to be bilinear isotropic for the stirrups placed in the beam. Bilinear isotropic material is also based on the von Mises failure criteria. The bilinear model requires the yield stress, as well as the hardening modulus of the steel to be defined.

For the tendons which are pre-stressed, it requires the multi-linear isotropic properties. The pre-stressing tendons was modelled using a multi-linear stress-strain curve developed using the following equations:

$$\varepsilon_{ps} \leq 0.008: f_{ps} = 28000\varepsilon_{ps}\ (ksi) \tag{3.4}$$

$$\varepsilon_{ps} > 0.008:\ f_{ps} = 268 - \frac{0.075}{\varepsilon_{ps} - 0.0065} < 0.98 f_{ps}(ksi) \tag{3.5}$$

Below is the stress-strain curve for the pre-stressing steel used in this study. Please check Appendix A for the related data.

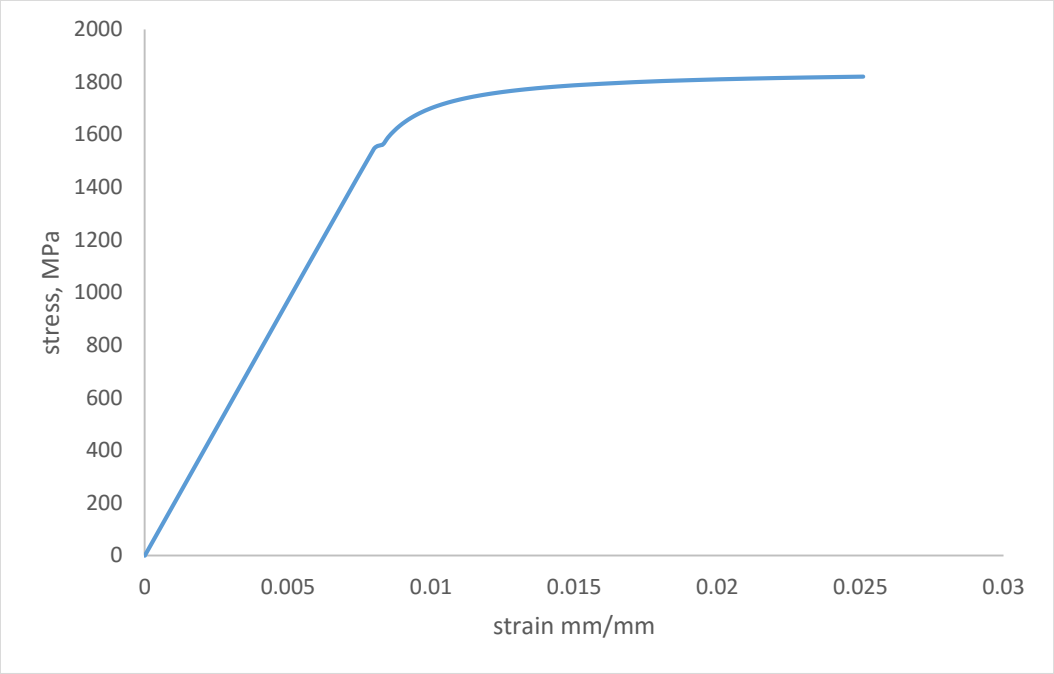

Figure 3.4: Stress-strain curve for pre-stressing steel

Table 3.3: Material Properties

Material 1 (Slab)		Material 2 (Beam)		Material 3 (Joist)	
Linear isotropic		Linear isotropic		Linear isotropic	
Ex	v	Ex	v	Ex	v
27000 MPa	0.2	33000 MPa	0.2	38000 MPa	0.2
Multi-linear isotropic		Multi-linear isotropic		Multi-linear isotropic	
Strain	Stress	Strain	Stress	Strain	Stress
0	0	0	0	0	0
0.000148148	4	0.000230303	7.6	0.000331579	12.6
0.000598148	12.4646	0.000780303	22.2094	0.001081579	38.2602
0.001098148	17.7248	0.001380303	32.7444	0.001681579	53.6192
0.001398148	19.3021	0.001780303	36.6238	0.002081579	60.2977
0.001798148	19.9999	0.002180303	37.9970	0.002481579	62.9942
Concrete properties		Concrete properties		Concrete properties	
Open	0.8	Open	0.4	open	0.4
Closed	0.8	Closed	0.8	closed	0.8
Cracking	1.6	Cracking	2.9	cracking	4.2
Crushing	1.2	Crushing	30	crushing	55

Material 4 (Column)		Material 5 (Tendons)		Material 6 (Stirrups)	
Linear isotropic		Linear isotropic		Linear isotropic	
Ex	v	Ex	v	Ex	v
100000 MPa	0.2	193050 MPa	0.3	200000 MPa	0.3
		Multi-linear isotropic		Bilinear isotropic	
		See Appendix A		Yield stress	250 MPa

3.2.5 Modelling

The combined slab-beam system modelled is provided in the structural design drawings presented in Appendix D. Figure B (See Appendix D) shows the portion of the whole slab-beam system that was chosen to be modelled in this study. The slab, beams, and columns were modelled as volumes. The combined volumes of the slab, beams, and columns are shown below. The dimensions of the slab is 6600 mm by 3800 mm with a height of 200 mm. The beams are 600 mm by 200 mm and the columns are 800 mm by 200 mm.

A T4-joist type (see Trasacco Group technical data in Appendix B) that represents a joist with 4 tendons was the joist type used in the slab-beam design and is what is modelled in this study. The joist sits on the beam 50 mm at both ends. The Link180 element were used to create the stirrups and tendons. The tendons are located inside the joist.

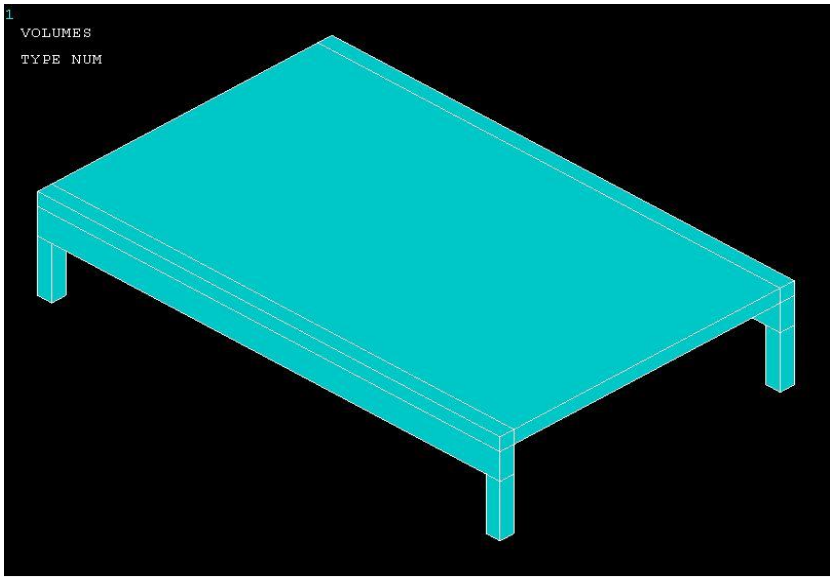

Figure 3.5: ANSYS volume model

3.2.6 Meshing

To get good results from the Solid65 element, the use of a rectangular mesh is recommended. Therefore, the mesh was set up such that square or rectangular elements with a maximum aspect ratio of 4 were created (Figure 3.6). The final meshed model used was obtained after various trials with different meshes. The final mesh had over 63,000 nodes and 57,000 elements. The final mesh used was arrived at taking convergence requirements and solution time into account. It must be noted that the finer the mesh, the longer the solution time. The final chosen mesh generally gave solution time of 2 days on a 64-bit 1.7 GHz quad core processor. The volume sweep command was used to mesh the various volumes. This properly sets the width and length of elements and nodes in the model.

The final meshed model is shown in Figure 3.6. The meshing of the stirrups and tendons is a special case compared to the volumes. No meshing of the stirrups and tendons was needed because individual elements were created in the modelling through the nodes created by the mesh of the concrete volume.

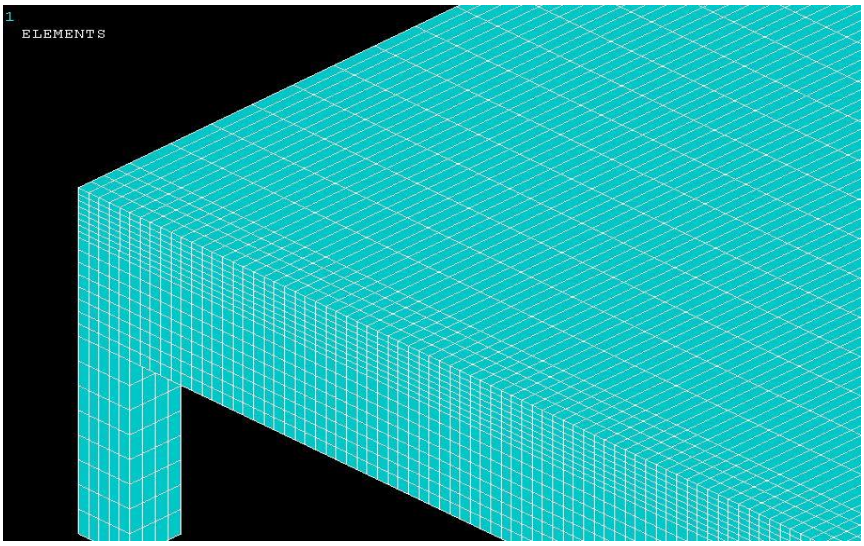

Figure 3.6: Meshed model

However, the necessary mesh attributes as described below needed to be set before each section of the stirrups and tendons was created. The element type number, material number, and real constant set number for the model were set for each mesh as shown below.

Table 3.4: Meshing Attributes for the FE model

Model parts	Element type	Material number	Real constant
Slab volume	1	1	1
Beam volume	1	2	1
Column volume	1	4	1
Stirrups and bar rod	2	6	3,4 and 5
Tendons	2	5	2
Joist	1	3	1

All three volumes were meshed with their corresponding materials. After meshing, some elements were modified to enable the joist be properly placed.

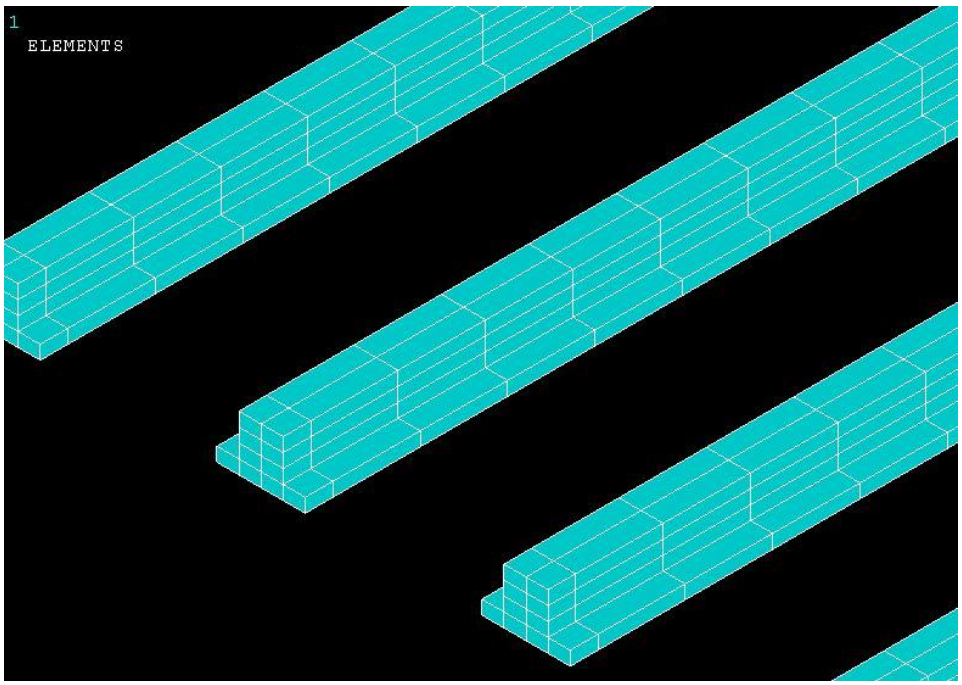

Figure 3.7: Zoom-in view of the T-shaped joists

The T-shape joist has a height of 100 mm with a breath of 150 mm and a length of 3900 mm. The joists rest on the beam before the hollow blocks were placed. For this model the hollow block were made to have the same material properties as the slab. Figure 3.8 shows the slab and joist only.

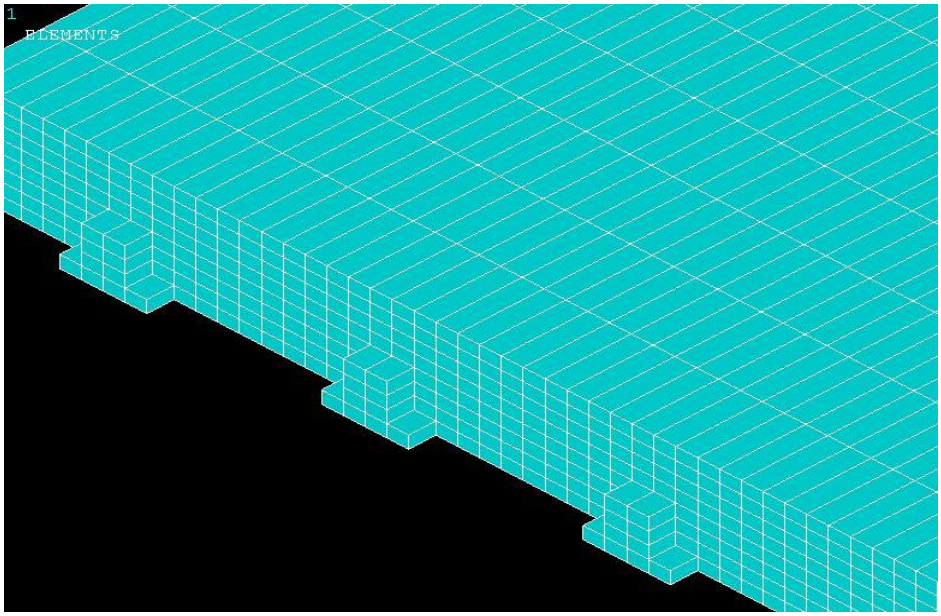

Figure 3.8: Slab and Joist system

A total of 14 T4 joists were used in this model with each having its own tendons. A T4 joist has four tendons but in this model only a tendon was used. The cross sectional area of the tendons were multiplied by 4 to represent the single tendon used. The stirrups were designed using the nodes of the beam and some part the steel bar extended into the slab from both ends. The stirrups and the beams are shown in figure 3.9 and 3.10.

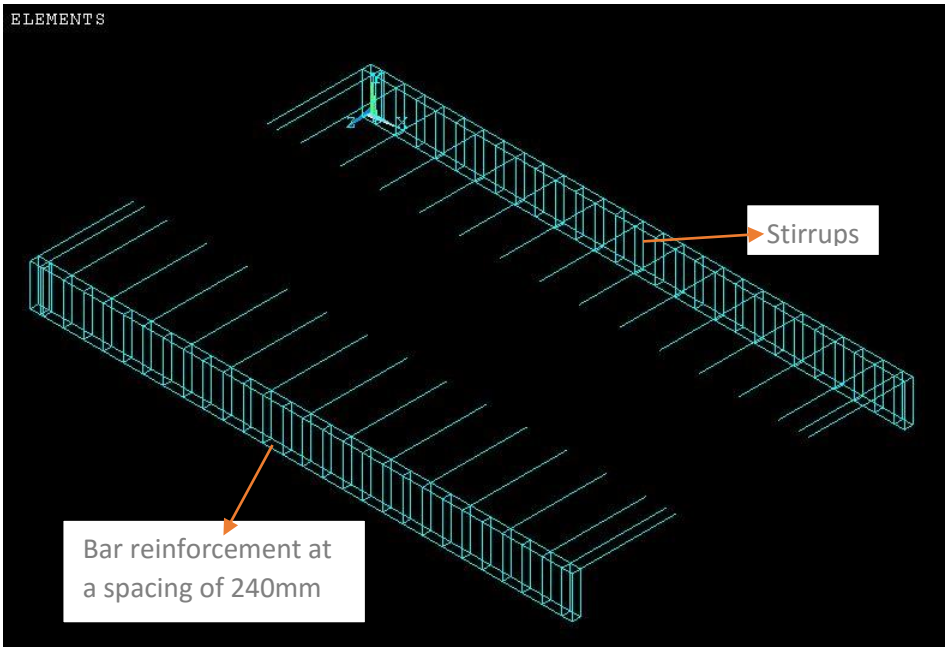

Figure 3.9: Beam stirrups and associated top steel

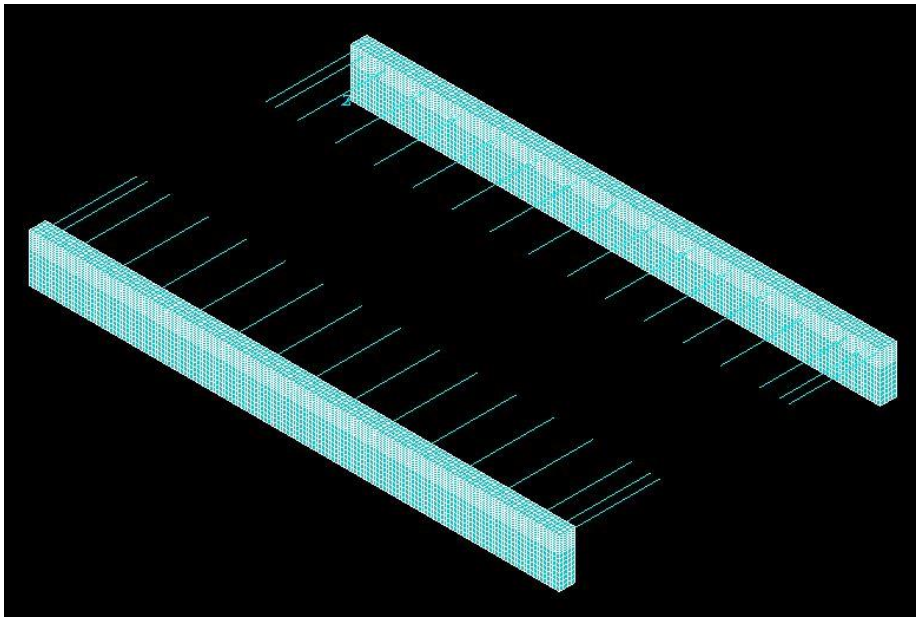

Figure 3.10: The beams together with stirrups

As mentioned earlier the joist sit on the beam 50 mm at both ends. In reality, the joint between the joist and the beam is not a fully fixed condition, however, for this initial

study, a fixed condition was assumed. The effect of partial fixity would be evaluated in a latter study. The assumed fixed end condition is expected to give a slightly stiffer response.

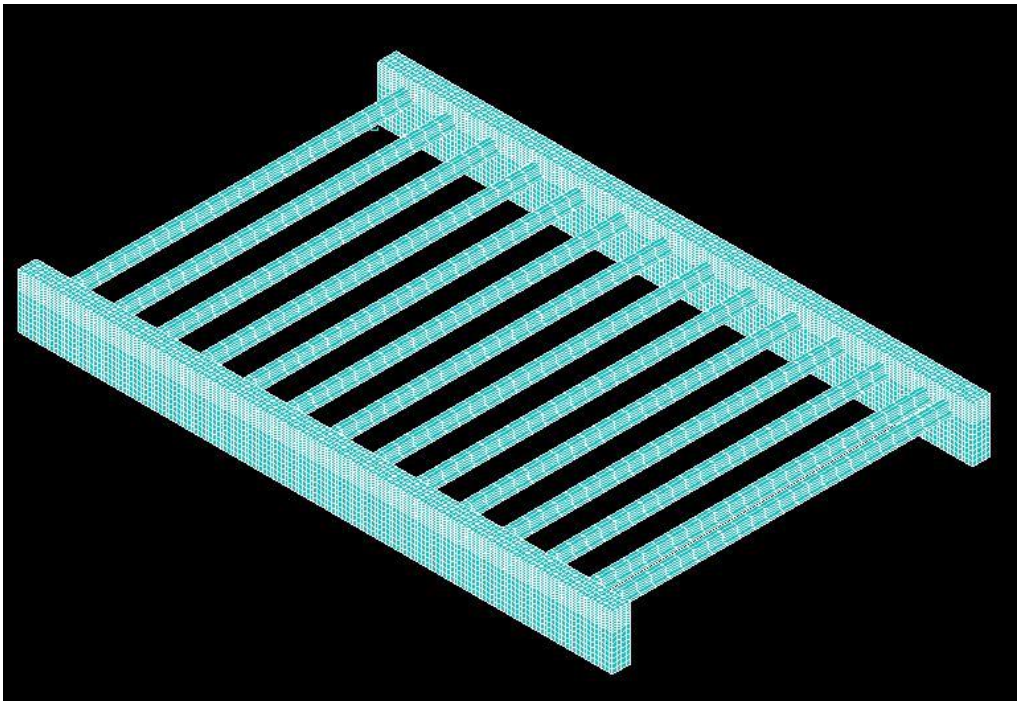

Figure 3.11: Combined beam and joist system

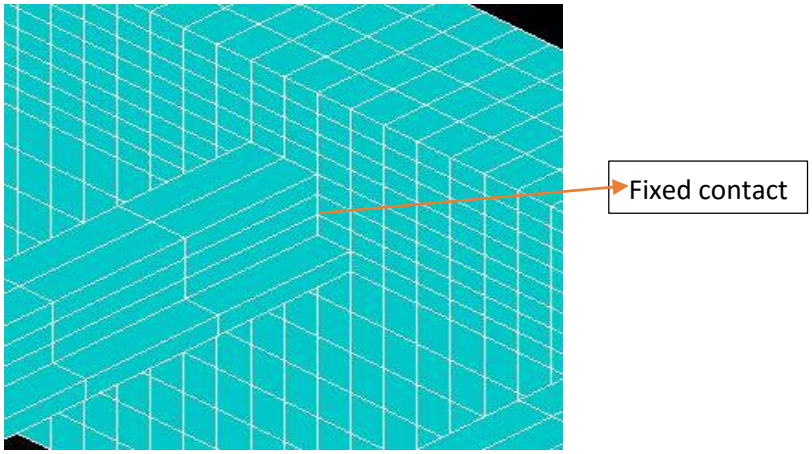

Figure 3.12: Fixed contact with the beam

3.2.8 Loads and Boundary Conditions

Displacement boundary conditions are needed to constrain the model to get a unique solution. If the model is not properly constrained, large displacement or stresses can occur, which interrupt the solution process. The model was constrained by fixing the nodes at the base of the column; i.e., applying zero translational movement (i.e. UX, UY and UZ is zero) at these nodes. See Figure 3.13 below:

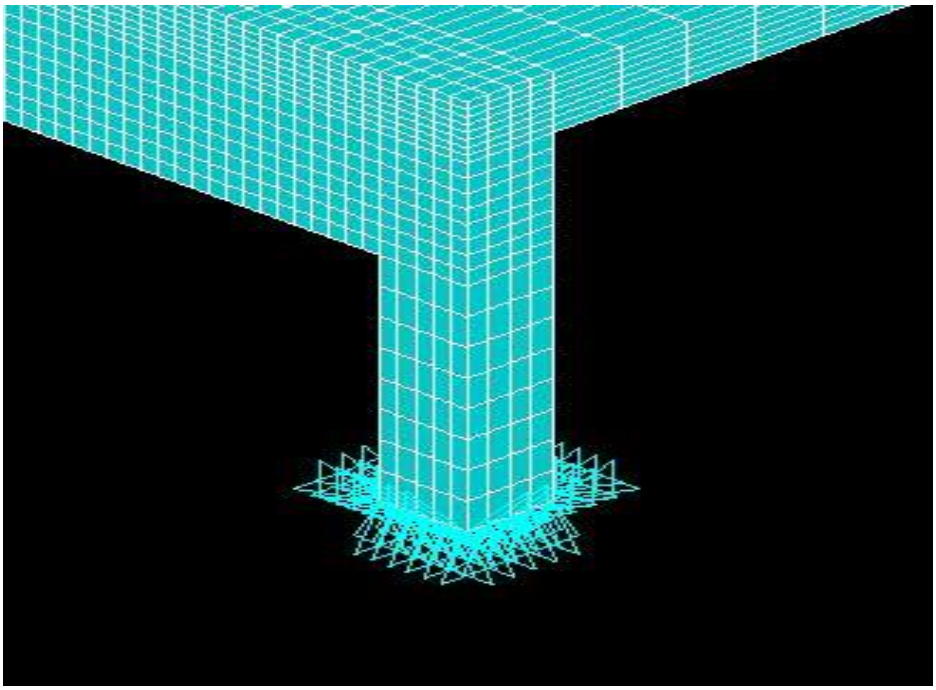

Figure 3.13: Translational boundary condition

3.2.9 Pre-stress

Unlike earlier versions of ANSYS in which the pre-stress loading is applied through a real constant by the defining initial strain, in Version 13, the pre-stress was applied with an initialization command code.

3.2.10 Analysis Type

For the purposes of the study the Nonlinear Static analysis type was chosen. The respective values of the various quantities representing the Solution Controls command for a nonlinear static analysis are shown in Table 3.5.

Table 3.5: Commands Used to Control the Analysis

Analysis option	Small displacement
Calculate Prestress effects	No
Time at end of Loadstep	1
Automatic time stepping	Prog chosen
Number of Substeps	4
Max no. of Substeps	4
Min no. of Substeps	4
Write items to result file	All solution items

The sub steps were set to indicate load increments used for the analysis. The program behaviour upon non-convergence for the analysis was set such that the program would terminate and exit. The rest of the commands were set to defaults. Two different solvers were used for the analysis. The sparse direct solver and the PCG (Pre-conditon CG) solver.

Sparse direct elimination solver is suited for analyses in which robustness and solution speed are required (nonlinear analyses), and for linear analyses in which iterative solvers are slow to converge (especially for ill-conditioned matrices, such as poorly shaped

elements). Handles models having 10,000 to 500,000 DOFs (more for shell and beam models).

The PCG (Pre-condition CG) iterative solver is suited for analyses in which solution speed is crucial, such as in linear analyses of large models. It is well-suited for bulky structures modelled with solid elements and can handles models having 50,000 to 1,000,000+ DOFs. The accuracy level can vary from 1 (fastest setting, fewer number of iterations) to 5 (slowest setting, accurate, more number of iterations) (ANSYS 2011).

3.2.11 The Newton-Raphson iteration

The Newton-Raphson (N-R) iteration is an iterative solution method using the concept of incremental step-by-step analysis to obtain the displacement u_i for a given load Pi. The N-R method keeps the load increment unchanged and iterates displacements and is therefore suitable to be used in cases when load values must be met. The N-R iteration can also be used for incremental increase of the deformation u. The search for the unknown deformation is described by the tangent of the load-displacement function. This is known as the tangent stiffness $k_{t,i}$ and describes the equilibrium path for each increment. The N-R iteration scheme is illustrated in Figure 3.14 which describes the search for the unknown deformation when a load is applied.

For the case where the initial deformation is u_0, the method according to which equilibrium is found can be described as follows. For the load increment ΔP_1 the corresponding displacement u_1 is sought. By means of the initial tangential stiffness $k_{t,0}$ the displacement increment Δu can be determined as:

$$\Delta u = {k_{t0}}^{-1} * \Delta P_1 \tag{3.6}$$

Adding this increment to the previous displacement u_0 gives the current estimate u_A of the sought displacement u_1 according to:

$$u_A = u_0 + \Delta u \tag{3.7}$$

The current error, or load imbalance, e_{PA} is defined as the difference between the desired force P_1 and the spring force (k*u_A) educed by the estimated displacement u_A. The stiffness k is evaluated from the tangent of the function at the point where u_A is found.

$$e_{PA} = P_1 - k.u_A \tag{3.8}$$

However, since the deformation has not been reduced by the current force P_1 this solution is not exact. If the error is larger than the limiting tolerance another attempt is made to find equilibrium. The new displacement increment Δu starting from the point a is calculated by means of the previous imbalance e_{PA}. Hence a displacement u_B closer to the desired u_1 is determined:

$$\Delta u = {k_{tA}}^{-1}.e_{PA} \tag{3.9}$$

$$u_B = u_A + \Delta u \tag{3.10}$$

Analogously, if the displacement u_B does not meet the tolerances for the load imbalance according to Eq. (3.8) yet another iteration within this load increment is carried out, now starting from point b. The iterations continue until the load imbalance approaches zero, the analysis then enters the next load increment ΔP_2 where these iterations are carried out until the load equilibrates to P_2 and the analysis has converged to a numerically acceptable solution u_2 for the load step.

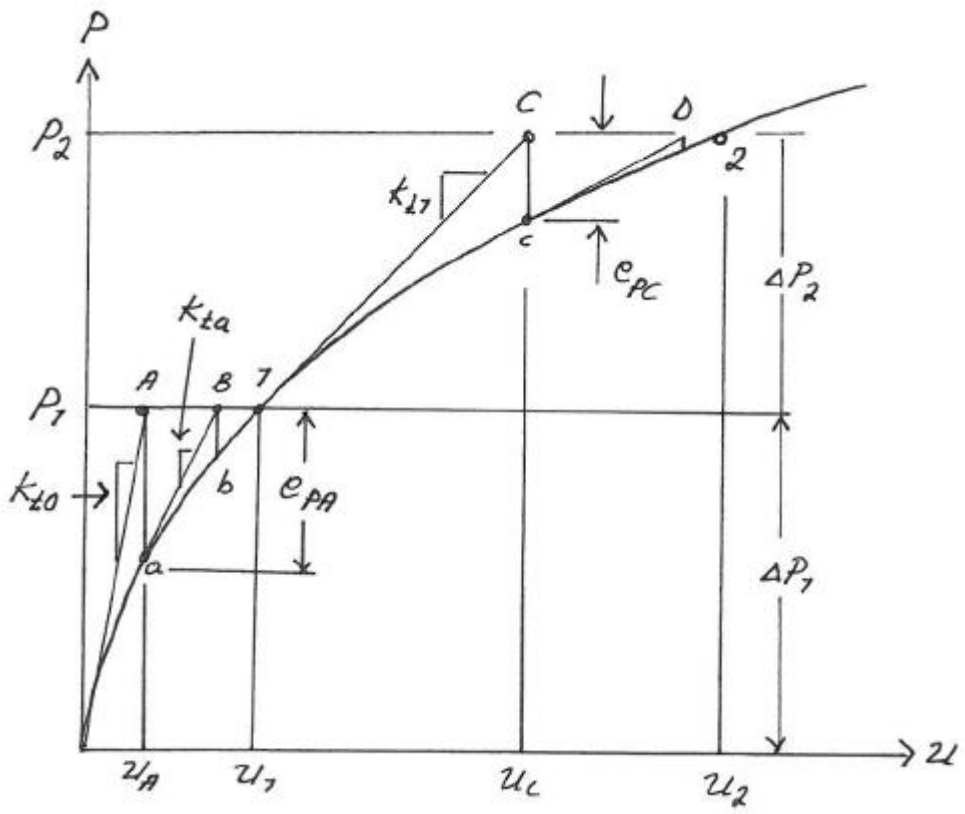

Figure 3.14: Newton-Raphson iteration scheme

Continued iterations normally cause force errors to decrease, succeeding displacement errors to approach zero and the updated solution to approach the correct value of the displacement. Moreover, smaller load increments can enhance the probability of finding equilibrium within each step.

The nonlinearity of the equations lies in the internal forces and the stiffness matrix having nonlinear properties. The stiffness matrix is deformation dependent and is therefore updated for each repetition. However, the recalculation of the stiffness matrix is very time consuming why this dependency can be neglected within a load increment in order to preserve linearity of the stiffness tangent. When neglected, the stiffness matrix is calculated based on the value of the deformations prior to the load increment. This simplification is

referred to as the modified Newton-Raphson iteration where the stiffness matrix is only updated for the first iteration in each step (see Figure 3.15). Apart from increasing computing pace, the drawback of this simplification is reduced accuracy.

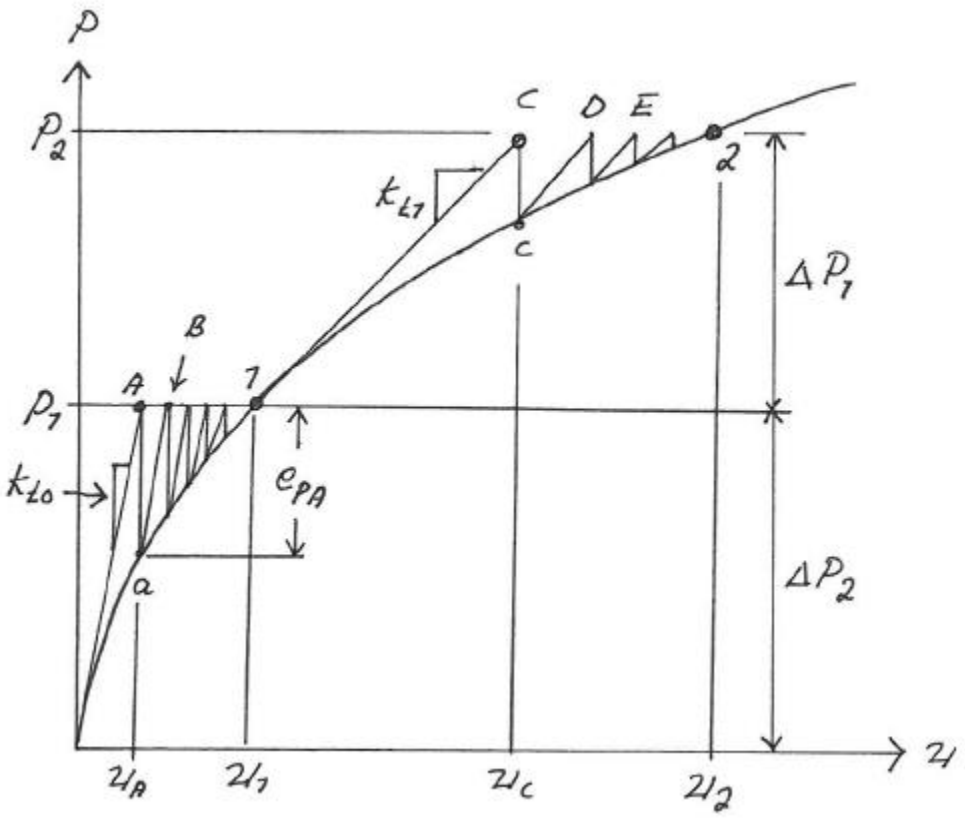

Figure 3.15: Modified Newton-Raphson iteration scheme

In the beginning of an analysis quite large load increments can be used. However, when the structure experiences significant loss of stiffness, normally during excessive crack propagation or when approaching failure load, increments need to decrease in order to achieve equilibrium. The use of smaller load increments can sometimes be insufficient since the stiffness reduction implies increasing deflections while loading decreases.

CHAPTER 4

RESULTS AND DISCUSSION

4.1 General

The non-linear response of the precast concrete slab modelled as per details discussed in Chapter 3 under incremental loading is presented in this section. The specific objective of this study is to understand how the combined mechanism of the beam-slab system actually works under the imposed loading regime and assess whether the precast concrete slab system can be used in light and heavy industrial infrastructure, e.g., for nuclear power plant construction.

In the analysis, surface loads has been applied on the surface of the slab and the load is gradually increased at each step till failure. The load-deflection curves are obtained from the analysis and the crack patterns at different load levels are observed.

4.2 Behavior at First Cracking

From the load deflection response (Fig. 4.5), the initial portion of the load deflection curve was due to the pre-stress in the joist. Comparisons were made in this region to ensure the stresses were consistent with the ANSYS model and Trasacco technical data. Once cracking occurs, deflections and stresses become more difficult to predict. The table below shows the stresses from the ANSYS model at 900 MPa pre-stress and the technical data:

Table 4.1 Pre-stress comparison

Materials	ANSYS model	Trasacco data
Joist concrete	$\sigma_t = +0.61$	$\sigma_t = +1.65$
	$\sigma_c = -1.56$	$\sigma_c = -2.09$
Tendons	900 MPa	1400 MPa

A phenomenon that occurred when the pre-stress was added was bursting in the concrete where the pre-stress force is being applied. This resulted in the first initial crack experience by the model (Fig. 4.1).

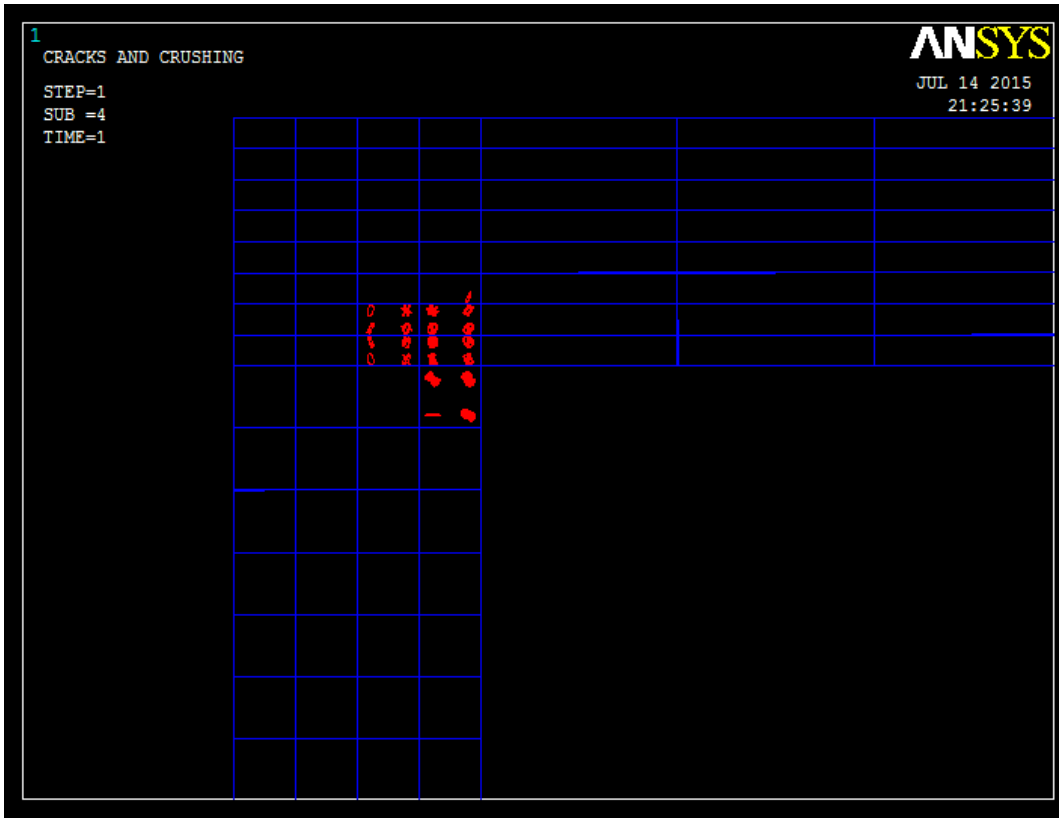

Figure 4.1: Initial crack due to pre-stressing

Also, cracking occurs in the base of beam at one end and no cracking was seen at the other end, as shown in Fig. 4.2. This is due to the double joist located at that end, resulting in the slab having more stresses in that region.

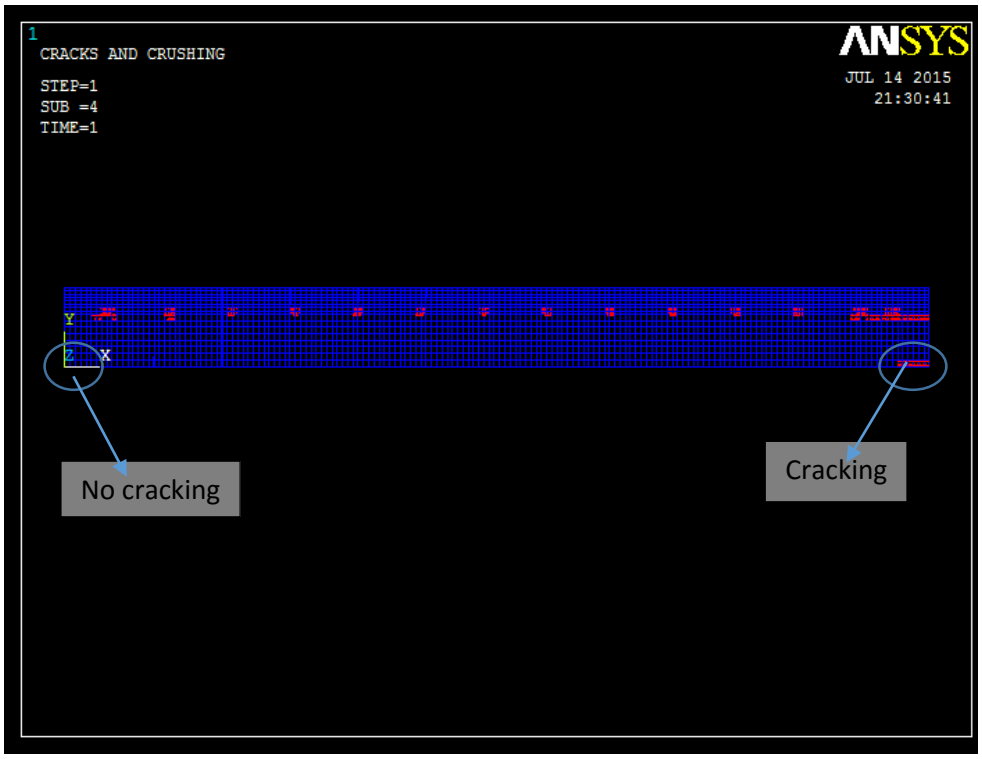

Figure 4.2: Cracking in the base of the beam after pre-stressing

4.3 Behavior beyond First Cracking.

In the non-linear region of the response, subsequent cracking occurs as more loads are applied to the ANSYS model. Cracking increases in the center of the beam at a surface load of 7.8 kPa. This intense cracking was also transferred to the slab up to a certain height. Flexural crack and diagonal tension cracks were observed. This cracking can be seen in Fig. 4.3.

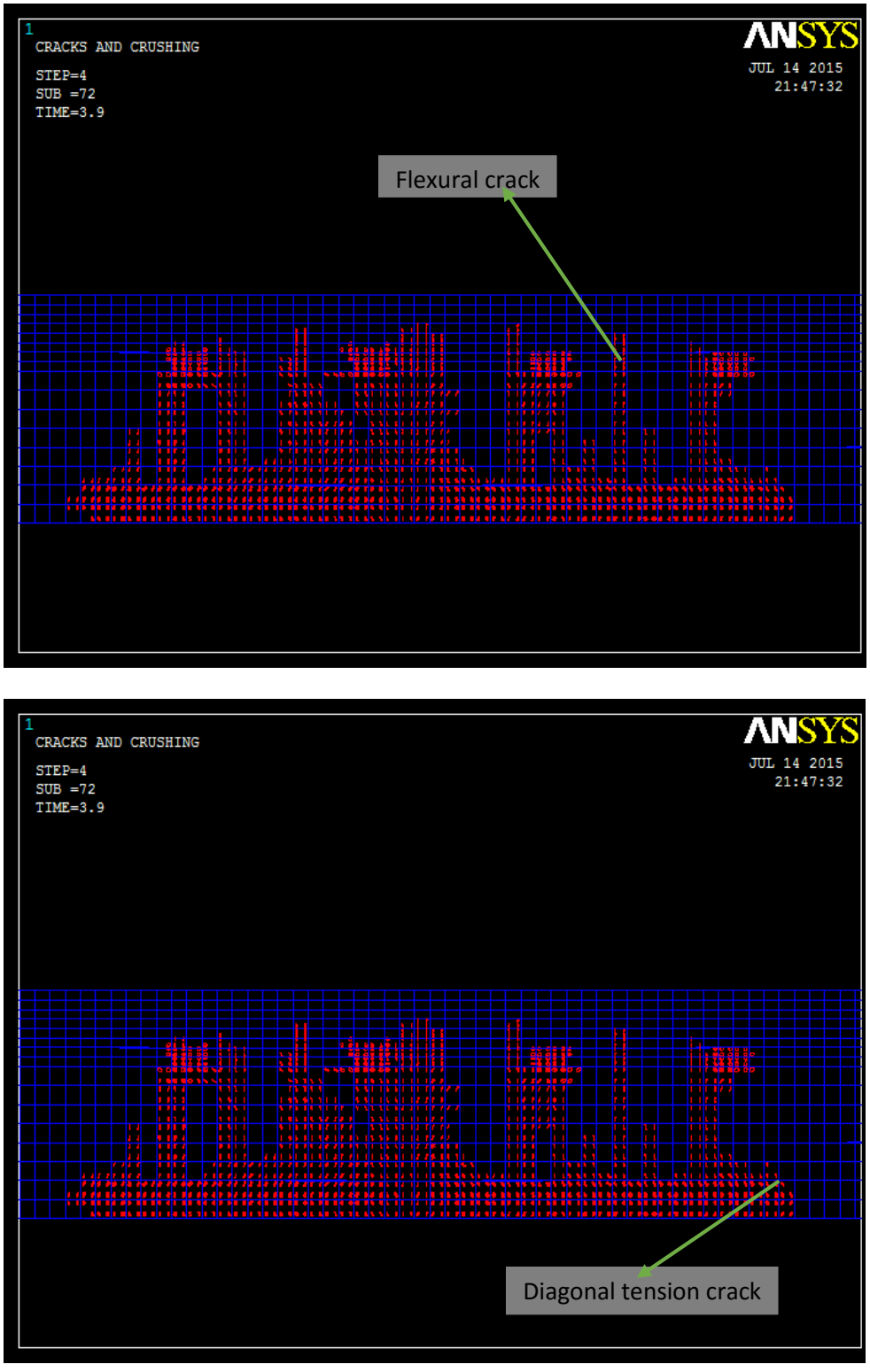

Figure 4.3 Flexural crack and diagonal tension crack

4.4 Behavior at Reinforcement Yielding

Steel reinforcement yielding in the slab occurred when a surface load of 13.5 kPa was applied. The cracked moment of inertia, yielding steel and nonlinear concrete material, now define the flexural rigidity of the concrete members. Therefore, greater deflections occur at the ANSYS model centerline.

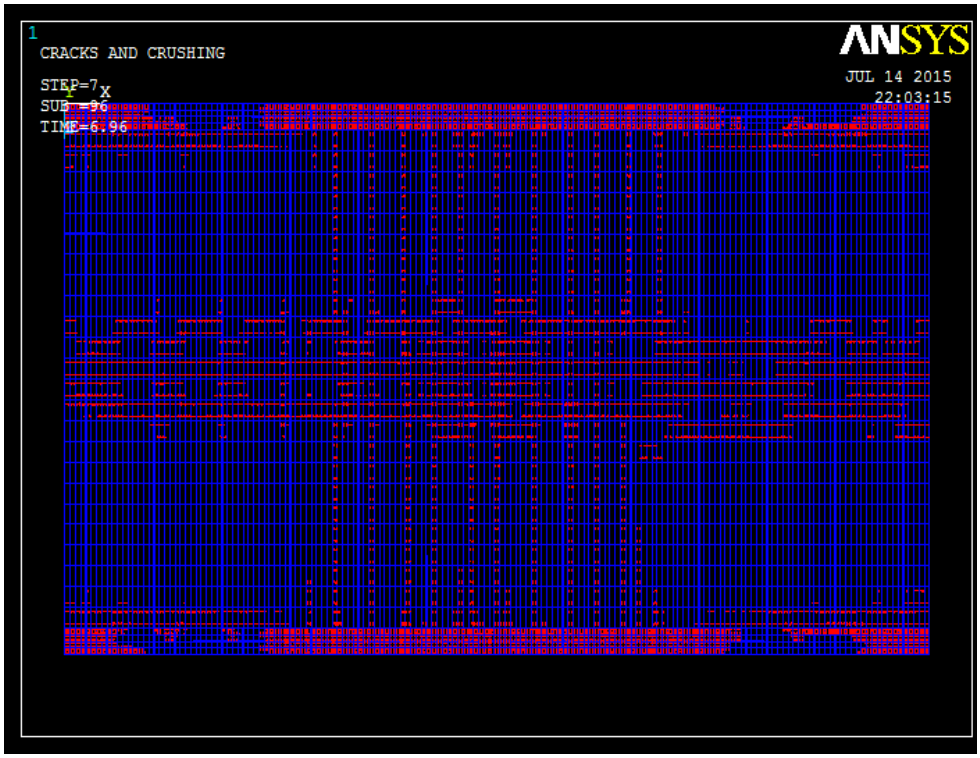

Figure 4.4: Cracking at yielding

4.5 Strength Limit State.

At a surface load of 14 kPa, the ANSYS model could no longer support additional load as indicated by the convergence failure. Severe cracking throughout the entire section at the constant moment region was noted at this point.

4.6 Load–Deflection Response.

Load–deflection behavior of concrete structures typically includes three stages. Stage I is the linear behavior of un-cracked elastic section. Stage II is the initiation of concrete cracking and Stage III relies relatively on the yielding of steel reinforcements and the crushing of concrete. ANSYS 13.0 utilizes Newton–Raphson method for the incremental load analysis. The load–deflection response for the analysis produced a similar behavior, which is shown in Fig. 4.5.

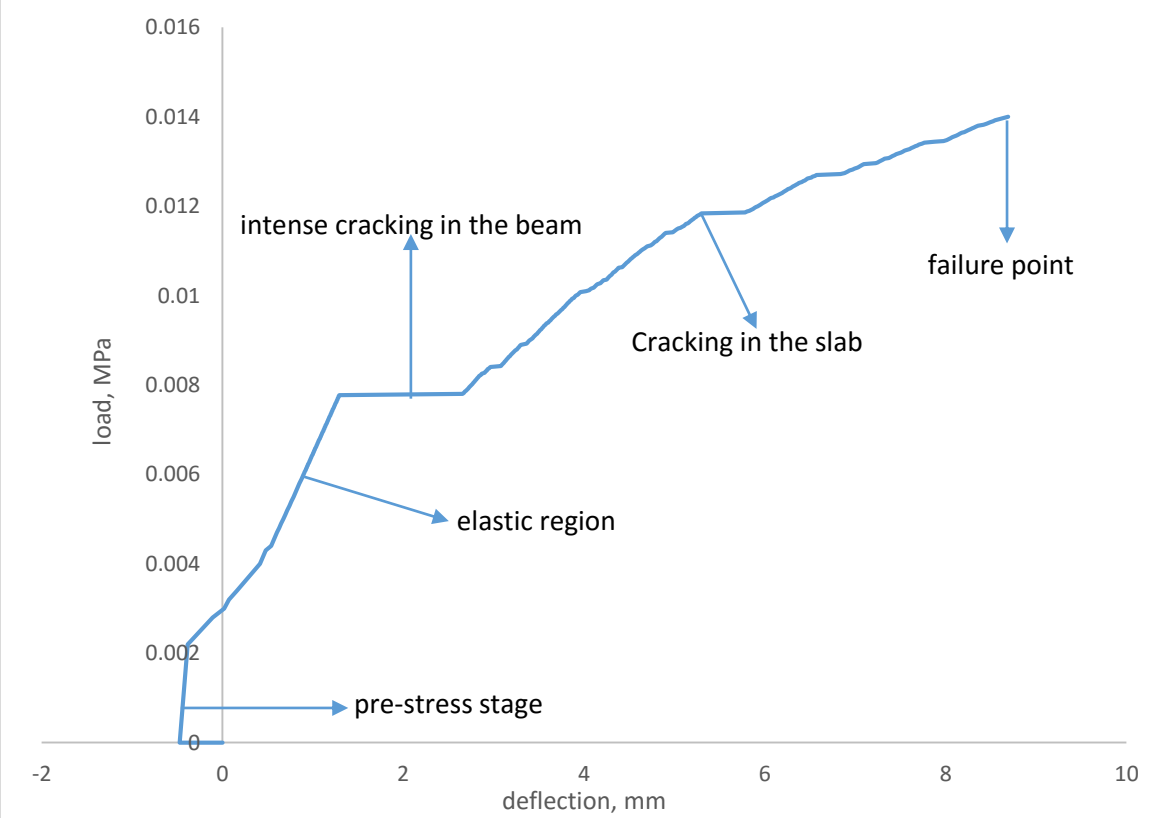

Figure 4.5: Load-deflection curve

4.7 ANSYS FE model, Design code and Trasacco data comparison

Comparisons regarding the service load and ultimate load for the ANSYS, model, EuroCode 2 Design Code, and the Trasacco technical data are shown in Table 4.2.

Table 4.2 Service load and Ultimate load comparison (in kPa)

	Service load	Ultimate load
FE model	9.9	13.8
Eurocode code	8.45	11.86
Trasacco data	9.12	13.2

The ANSYS FE model service loads are estimated as the load at which cracking starts in the slab, the ultimate load is taken as the point at which the model fails. From the table, the service load and the ultimate load in the ANSYS model are slightly higher than both loads from the Eurocode design and Trasacco data. However, the comparison is noted to be satisfactory and it can be noted that the ANSYS FE model is very capable of predicting the nonlinear response of the Trasacco floor system.

Noting that the T4 joist system used for this study is providing loads that are for office buildings, and noting the difference between the service moment capacities between this and the double-joist systems with 7 strands: That is, from Appendix B, it can be noted that the service moment for a 200 mm thick slab with T4 joists is 16.46 kNm, however, the service moment for a 250 mm slab with double T7 joists is 54.54 kNm. This represents about a 3x increment in the moment capacity.

Comparing this to the live load values for light to heavy industrial structures given in Table 2.1 that ranges from 6 – 11.97 kPa, to that of office buildings that ranges from 2 – 3.0 kPa (BS EC1, 2002), it can be inferred that the Trasacco fast floor can be used for light and heavy industrial structure like the nuclear facilities.

The information on the calculation of the service and ultimate load is presented in Appendix C.

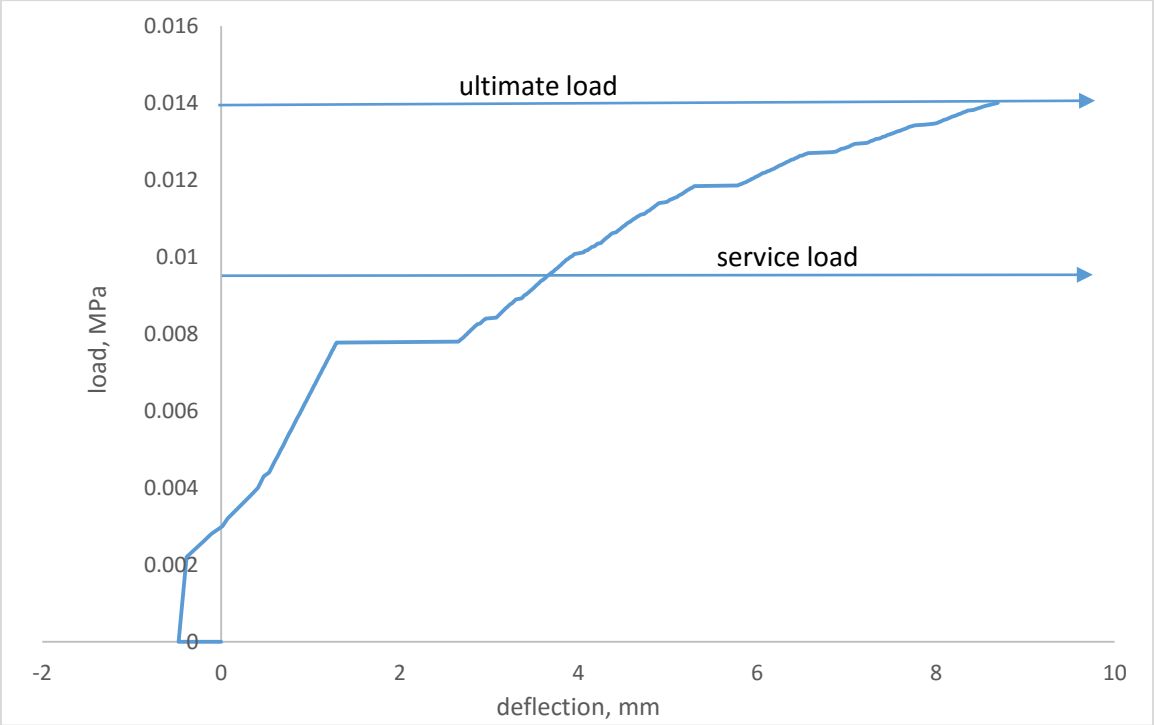

Figure 4.6: Load-deflection curve showing the service and ultimate load

CHAPTER 5

CONCLUSIONS AND RECOMMENDATIONS

The purpose of this research was to understand the behaviour of a precast concrete slab system under monotonic loading condition. A finite element model capable of simulating the nonlinear response of the Trasacco precast concrete slab was modelled using ANSYS structural.

The main concerned of the research was predicting the load-deformation behaviour and crack pattern for a precast concrete slab. Numerical comparisons between the ANSYS model and the Trasacco group floor data have also been carried out.

CONCLUSIONS

The main conclusions that can be drawn from this study in answer to the objectives for which this finite element assessment was conducted are presented below as follows:

1. The finite element model used in this present study is clearly capable of simulating the nonlinear behaviour of the Trasacco precast concrete slab under monotonic vertical loading.
2. The results reveal the accuracy and efficiency of the developed ANSYS 13 model in predicting the load-deformation behaviour and crack pattern.
3. With the imposed live loads mentioned in Chapter 2 for light and heavy industrial structures (typical of nuclear facilities), the comparison of the results of the model with the British EuroCode design manual and the Trasacco group floor data, shows the potential for the floor system (e.g., the double joist system) to be used for these types of structures.

RECOMMENDATION

The following are the recommendations for future work:

1. Further analysis should be performed on a two bay slab system since this study focussed on a single bay slab system.
2. It is important that analysis is conducted to assess the monotonic horizontal load – deformation response, as would occur under extreme seismic action. This can be conducted by assessing the case of a horizontal uniform load for a slab-wall connection.
3. It is also important to conduct this same study for the case of the double joist system.
4. Lastly, a full model of a typical nuclear facility with the fast floor system, can be analysed under the various loading conditions in order to assess the response.

REFERENCE

ANSYS. (2011). ANSYS, Mechanical APDL Theory Reference (Release 13.0)

ASCE Task Committee on Finite Element Analysis of Reinforced Concrete Structures (1982). State-of-the-Art Report on Finite Element Analysis of Reinforced Concrete, ASCE Special Publications.

ASCE, 2005. "Minimum Design Loads for Buildings and Other Structures"- ASCE 7 05, American Society of Civil Engineers, New York, 2005.

Barbosa, A.F. and Ribeiro, G.O. (1998). "Analysis of Reinforced Concrete Structures using ANSYS Nonlinear Concrete Model", in Computational Mechanics -New Trends and Applications, Barcelona, Spain, pp. 1-7.

Bazant, Z.P. and Cedolin, L. (1983). "Finite Element Modelling of Crack Band Propagation". Journal of Structural Engineering, ASCE, Vol. 109, No. 1, pp. 69-93.

Bazant, Z.P. and Oh, B.H. (1983). "Crack Band Theory for Fracture of Concrete". Materials and Structures, RILEM, Paris, Vol. 16, pp. 155-176.

Barzegar, F. and Schnobrich, W.C. (1986). "Nonlinear Finite Element Analysis of Reinforced Concrete under Short Term Monotonic Loading". Civil Engineering Studies SRS No. 530, Univ. of Illinois at Urbana, Illinois.

Bjarnason, J. O. (2008). "Pushover analysis of an existing reinforced concrete structure". School of science and engineering, Reykjavik University, Iceland.

BS EC1 (2002). Eurocode 1: Actions on structures - Part 1-1: General actions Densities, self-weight, imposed loads for buildings, British Standards Institution.

BS EC2 (2004). Eurocode 2: Design of concrete structures - Part 1-1: General rules and rules for buildings, British Standards Institution.

Dotroppe, J.C., Schnobrich, W.C. and Pecknold, D.A. (1973). "Layered Finite Element Procedure for Inelastic Analysis of Reinforced Concrete Slabs". IABSE Publication, Vol. 33-11.

Fanning, P. (2001), "Nonlinear Models of Reinforced and Post-tensioned Concrete Beams", Electronic Journal of Structural Engineering, University College Dublin, Earlsfort Terrace, Dublin 2, Ireland, Sept.12.

Fib. (2007). FRP reinforcement in RC structures, The international Federation for Structural Concrete, Bulletin 40. Lausanne. Switzerland.

Fib. (2012a). Modal Code 2010 – final draft, Volume 1, The international Federation for Structural Concrete, Bulletin 65. Lausanne. Switzerland.

Gilbert, R.I. and Warner, R.F. (1978). "Tension Stiffening in Reinforced Concrete Slabs". Journal of Structural Division, ASCE, Vol. 104, No. ST12, pp. 1885-1900.

John D. Stevenson and Ovidiu coman (2006), *Design of hazardous mechanical structures, systems and components for extreme loads*, ASME press, New York, USA.

Kachlakev, D.I.; Miller, T.; Yim, S.; Chansawat, K.; Potisuk, T. (2001), "Finite Element Modelling of Reinforced Concrete Structures Strengthened With FRP Laminates", California Polytechnic State University, San Luis Obispo, CA and Oregon State University, Corvallis, OR for Oregon Department of Transportation, May.

Kwak, H.G. (1990). "Material Nonlinear Finite Element Analysis and Optimal Design of Reinforced Concrete Structures". Ph.D. Dissertation, Department of Civil Engineering, KAIST, Korea.

Leibengood, L.D., Darwin, D. and Dodds, R.H. (1986). "Parameters Affecting FE Analysis of Concrete Structures", Journal of Structural Engineering, ASCE, Vol. 112, No. 2, pp. 326-341.

Liu, G. R., & Quek, S. S. (2003). *The Finite Element Method: A Practical Course*. Oxford: Butterworth-Heinemann.

McCurry, D., Jr. and Kachlakev, D.I (2000), "Strengthening of Full Sized Reinforced Concrete Beam Using FRP Laminates and Monitoring with Fiber Optic Strain Guages" in Innovative Systems for Seismic Repair and Rehabilitation of Structures, Design and Applications, Technomic Publishing Co., Inc., Philadelphia, PA, March.

Meyer, C. and Okamura, H. (1985). "Finite Element Analysis of Reinforced Concrete Structures". Proceedings of the US-Japan Joint Seminar on Finite Element Analysis of Reinforced Concrete, Tokyo, Japan.

Neville, A.M., & Brooks, J.J. (2008). *Concrete technology*. Harlow, Essex, UK: Pearson Prentice Hall.

Nawy, E.G., (2000), *Prestressed Concrete: A Fundamental Approach*, Prentice-Hall, Inc., Upper Saddle River, NJ.

Nawy, E.G., (2009), *Prestressed Concrete* (5^{th} ed). Prentice-Hall, Inc., Upper Saddle River, NJ.

Zhang Q. and Hussain A. (2004). "Modelling slab column connections reinforced with GFRP under localized impact", Research Report, Memorial University of Newfoundland, St.John"s Canada, pp.1-12.

Rashid, Y.R. (1968). "Analysis of Prestressed Concrete Pressure Vessels". Nuclear Engineering and Design, Vol. 7, No. 4, pp. 334-344.

Scanlon, A. and Murray, D.W. (1974). "Time Dependent Reinforced Concrete Slab Deflections". Journal of the Structural Division, ASCE, Vol. 100, No. ST9, pp. 1911-1924.

Strescon (2014). Trasacco Floor Structural Design Drawings for TAYSEC Apartments, Strescon Engineering Consultancy Limited.

Tavarez, F.A., (2001), "Simulation of Behaviour of Composite Grid Reinforced Concrete Beams Using Explicit Finite Element Methods", Master's Thesis, University of Wisconsin-Madison, Madison, Wisconsin.

Trasacco Group (2005). "Floor Slab with Prestressed Concrete Joists and Hollow Blocks: Single Joist and Double Joist", Trasacco Group Publication.

Willam, K.J. and Warnke, E.P. (1974), "Constitutive Model for Triaxial Behaviour of Concrete", Seminar on Concrete Structures Subjected to Triaxial Stresses, International Association of Bridge and Structural Engineering Conference, Bergamo, Italy, p.174.

APPENDIX A

STRESS-STRAIN CURVE INFORMATION

Concrete C12 properties

Mean compressive strength	f_{cm}	20 MPa
Mean tension strength	f_{ctm}	1.6 MPa
Secant modulus	E_{cm}	27000 MPa
Strain at peak stress	ε_{c1}	0.0018

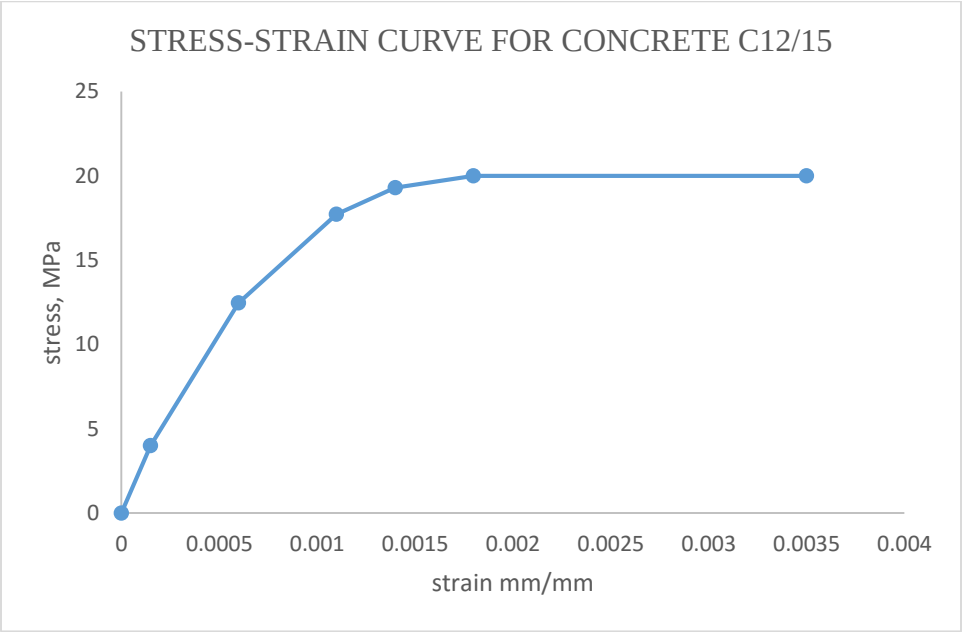

Concrete C30 properties

Mean compressive strength	f_{cm}	38 MPa
Mean tension strength	f_{ctm}	2.9 MPa
Secant modulus	E_{cm}	33000 MPa
Strain at peak stress	ε_{c1}	0.0022

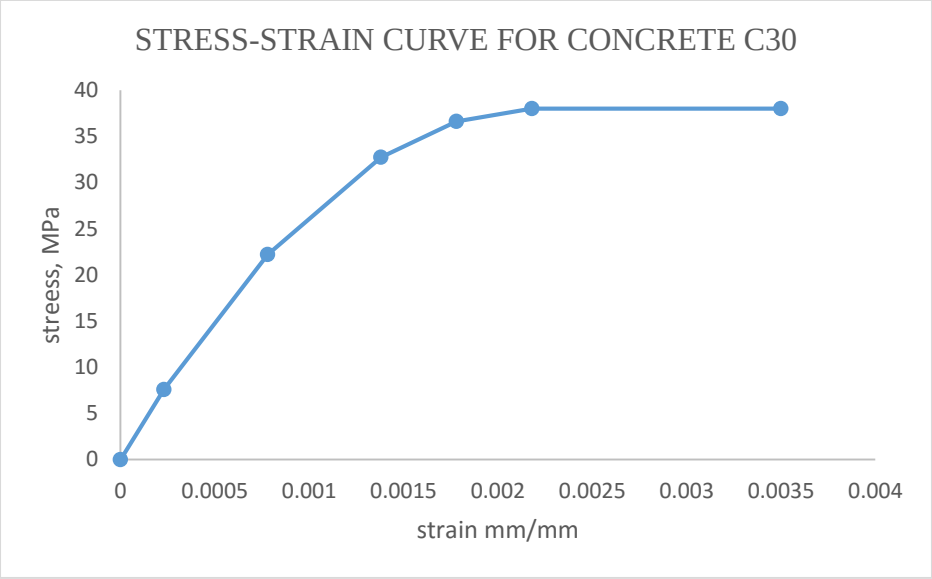

Concrete C/55 properties

Mean compressive strength	f_{cm}	63 MPa
Mean tension strength	f_{ctm}	4.2 MPa
Secant modulus	E_{cm}	38000 MPa
Strain at peak stress	ε_{c1}	0.0025

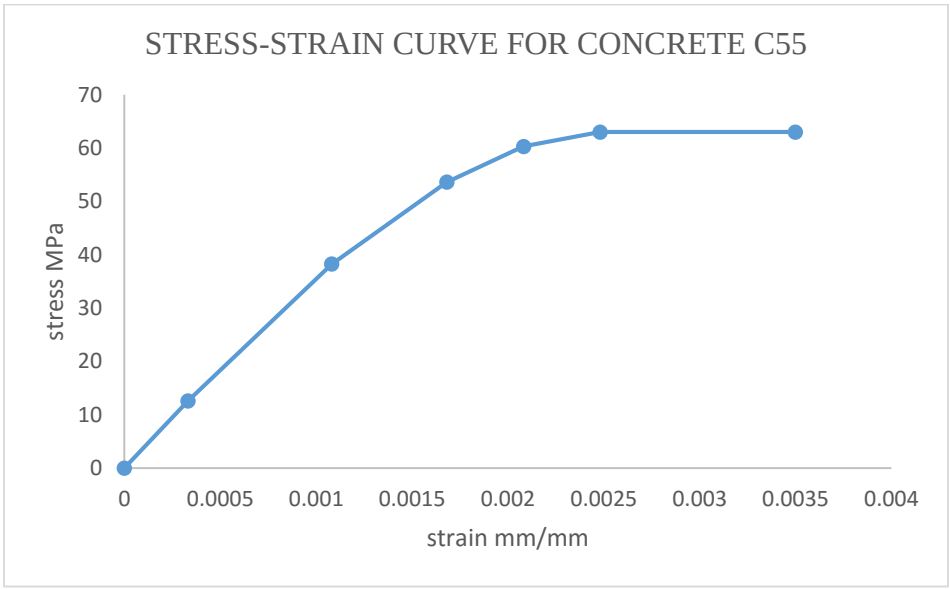

PRE-STRESSING STEEL DATA

Strain	Stress, MPa
0	0
0.008	1544.426
0.0083	1560.513
0.0085	1589.241
0.0087	1612.746
0.0089	1632.334
0.0091	1648.908
0.0093	1663.114
0.0095	1675.426
0.0097	1686.199
0.0099	1695.705
0.0101	1704.154
0.0103	1711.714
0.0105	1718.518
0.0107	1724.674
0.0109	1730.271
0.0111	1735.38
0.0113	1740.064
0.0115	1744.374
0.0117	1748.351
0.0119	1752.034
0.0121	1755.454
0.0123	1758.639
0.0125	1761.61
0.0127	1764.391
0.0129	1766.997
0.0131	1769.445
0.0133	1771.75
0.0135	1773.922
0.0137	1775.974
0.0139	1777.916
0.0141	1779.755
0.0143	1781.499
0.0145	1783.157
0.0147	1784.733
0.0149	1786.235
0.0151	1787.666

0.0171	1799.011
0.0191	1806.755
0.0211	1812.377
0.0231	1816.644
0.0251	1819.993
0.0271	1822.693
0.0291	1824.914
0.0311	1826.774
0.0331	1828.355
0.0351	1829.714
0.0371	1830.896
0.0391	1831.933
0.0411	1832.85
0.0431	1833.666
0.0451	1834.398
0.0471	1835.058
0.0491	1835.656
0.0511	1836.201
0.0531	1836.698
0.0551	1837.155
0.0571	1837.575
0.0591	1837.964

APPENDIX B

TRASACCO FAST FLOOR DESIGN SHEET

FLOOR SLAB WITH PRESTRESSED CONCRETE JOISTS AND HOLLOW BLOCKS

SINGLE JOIST AND DOUBLE JOIST

Product destination

It is intended for a rapid and economical building of floor slabs made by pre-stressed concrete beams and cement hollow blocks. The beams are industrially mass-produced for prompt delivery in spans multiple of cm 20 starting from 1.20 m up to 7.60 m.

Description

The floor slab is made by 12 x 9 cm beams in pre-stressed reinforced concrete in adherent threads reinforced with a minimum of three strands up to a maximum of seven strands 3 x 2.25 of 11.93 sqmm section each interposed by cement hollow blocks of 38 x 25 cm with a depth varying from 12 up to 20 cm.

The floor slab is completed by a finishing concrete cast in situ which, according to the static conditions, can have on top of a maximum thickness of 5 cm.

MATERIALS	BREAKING STRESSES N/sqmm	SAFE STRESSES N/sqmm
JOISTS CONCRETE	Rck > 55	$\bar{\sigma}t = +1.65$ $\bar{\sigma}c = -2.09$
CONCRETE CAST IN SITU	Rck ≥ 25	$\bar{\sigma}c = 8.5$ $\bar{\tau}co = 0.533$
TENDONS	1800	1400

Material features

Joists characteristics table

JOISTS CHARACTERISTICS 9/12 Weigh 0.18 kN/m	T3	T4	T5	T6	T7	N°	Distinctive sign identifying reinforcement type
	0.36	0,48	0,60	0.72	0,84	Ap=sqcm	Area of prestressing tendons
	-1.349	-2.715	-3.871	-3.940	-4.090	σcps N/sqmm	Concr. compr.ve prestress at top of joist section
	-8.54	-10.50	-12.49	-15.54	-17.14	σcpi N/sqmm	Concr. compr.ve prestress at bott. of joist section
	5.52	5.54	5.55	5.56	5.57	xi=cm	Ideal area from upper edge barycentric distance
Section area B=72 sqcm	453	457	457	459	461	Ji=cm⁴	Ideal area joist barycentric moment of inertia

Having located the external exercise stress Me –positive and negative – and Te calculated according to the usual elastic theory methods, the project calculation is reduced to the solution table finding for which have been respected at the same time conditions Ms>=Me – at positive and negative – and Ts>=Te.

Directions:

For the storage of pre-stressed concrete joists

The joists must be piled by putting in between each layer wooden strips. The strips must be positioned at maximum distance of 100 cm from each other.

It is absolutely necessary that ground on which the piles are laying is levelled and compacted. Above all it is very important that the wooden strips are positioned on the same vertical line.

Transport and assembly

The lifting of the beams must take avoiding jerks or shoves, making sure that the base of the beam is always facing downwards. The distance between the couplings must not exceeding 2 mt and the space between each layer must not be more than 1.50 mt.

Lay down the divider strips before casting the slab at distance not exceeding 2 mt. In any case it is advisable to foresee at least one in the middle. For floor slabs weighing more than 2.5 kN/sqm reduce in accordingly such distance. The uprights must be stiff sufficiently braced, paying particular attention to the top struts.

Penetration of the beams on the supports

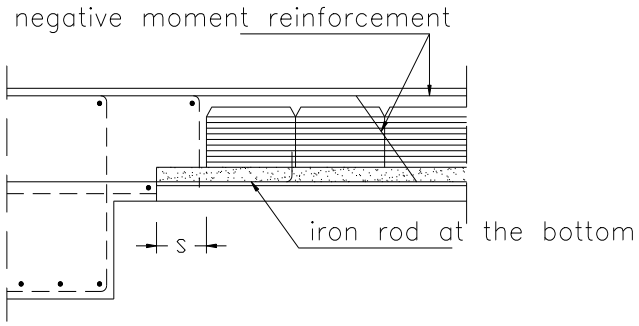

The correct positioning and the foreseen centre distance of the beams is obtained by setting out at each and spacing blocks.

In case of laying on top on walls or of overhanging architrave a beam penetration of 5-10 cm is sufficient. When there are flush support (beam of the same thickness of the slab or T- shaped architraves' wings) the S penetration in cm must be of:

- For single beam slab $S \geq T/100$

- For double beam slab $S \geq T/140$

where T is the shear stress in kN/ml.

Depending on the type of support (especially for the beams of the same thickness of the slab or T-shaped architraves 'wings) it is necessary to add a lower reinforcement (segment or brackets) suitable for a tensile stress equal to the shear and adequately anchored.

Avoid concentrated weights (i.e. piles of blocks) in the areas not reinforced by divider strips.

For the transversal distribution.

For flor slabs with a span more than 4.5 mt or when there are irregular spaces, it is necessary to foresee the realisation of one or more dividing ribbing, by using the end block. The reinforcement of such ribbing must be made of at least 4 ϕ 10 and brackets ϕ 5 placed at a maximum distance of 25 cm Floor slab must be foreseen a reinforced equal to at least 3 ϕ 6 in perpendicular direction of the beams..

Cast concrete in situ supplementary instructions

Floor slab and integrative casting to be made with C 250 concrete unless othervise specified.Lay down the walking planks.

Before casting,the bricks and the beams must be cleaned and thoroughly wetted;vibrate accurately the casting and make sure that the ribbing are well stuffed.

The aggregate grading must be appropriate, with a maximum dimension of 12 mm and casting must be compacted to guarantee the wrapping of the reinforcements and the adherence between blocks and beams. Water/cement ratio approximately 0.5.

Additional reinforcement

The supplementary reinforcement (of tensile stress, for negative moments) must be placed at the time of casting in correspondence to the beams so that it is covering will be about 2 cm from the top edge of the finished slab.

Dismantling instructions

The striking centres must take place in steps and in such a way to avoid dynamic actions. In addition it must not be done before the concrete resistance will have reached the necessary value according to the use.

Minimum suggested striking time for concrete C 25 is 20 days.

ITAL PRESTRESS & CONSTRUCTION PRODUCTS
P.O.Box MD 663,Accra,Ghana Tel: 302655 Fax: 660074 E-mail: ital@ighmail.com

PRESTRESSED CONCRETE FLOOR

JOISTS FEATURES

JOISTS CHARACTERISTICS	T3	T4	T5	T6	T7	N°	Distinctive sign identifying reinforcement type
Weigh 0.18 kN/m	0.36	0,48	0,60	0.72	0,84	Ap=sqcm	Area of prestressing tendons
	-1.349	-2.715	-3.871	-3.940	-4.090	σcps N/sqmm	Concr. compr.ve prestress at top of joist section
	-8.54	-10.50	-12.49	-15.54	-17.14	σcpi N/sqmm	Concr. compr.ve prestress at bott. of joist section
	5.52	5.54	5.55	5.56	5.57	xi=cm	Ideal area from upper edge barycentric distance
Section area =72 sqcm	453	457	457	459	461	Ji=cm⁴	Ideal area joist barycentric moment of inertia

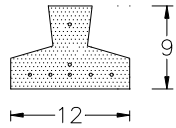

SINGLE JOIST i=50 cm

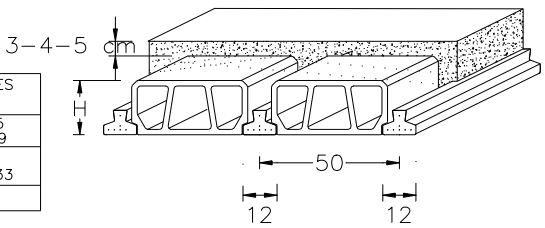

MATERIALS FEATURES

MATERIALS	BREAKING STRESSES N/sqmm	SAFE STRESSES N/sqmm
JOISTS CONCRETE	Rck > 55	σ̄t = + 1.65 σ̄c = - 2.09
CONCRETE CAST IN SITU	Rck ≥ 25	σ̄c = 8.5 τ̄co= 0.533
TENDONS	1800	1400

THICKNESS AND WEIGTH FLOOR DATA				TECHNICAL DATA REFERRED TO 1 mt SPAN FLOOR STRIP											
				PARTIAL SECTION				ALL REAGENT SECTION			Me SERVICEABLE POSITIVE MOMENTS kN m				
						MOD. RESIST.					TENDONS JOISTS TYPE				
HOLLOW POT THICKNESS	CONCRETE THICKNESS	CONCRETE QUANTITY	SELF WEIGHT IN SITU	NEUTRAL AXIS	MOMENT OF INERTIA	UPPERSIDE	UNDERSIDE	BARYCENTRIC AXIS DISTANCE	SECTION AREA	BARYCENTRIC MOM. OF INERTIA					
H cm		l/m²	kN/m²	x cm	J cm⁴	Ws cm³	Wi cm³	Xc cm	Ac cm²	Jc cm⁴	T3	T4	T5	T6	T7
12	+3	46	2.30	5.29	14577	2755	1001	6.76	985	22293	8.12	11.16	14.12	16.35	19.20
	+4	56	2.55	5.52	17493	3171	1112	7.09	1085	27087	8.84	12.15	14.93	18.00	20.99
	+5	66	2.80	5.78	20683	3577	1229	7.45	1185	32373	9.57	13.12	16.13	19.48	22.71
16	+3	58	2.70	6.69	29682	4436	1545	8.94	1186	46846	10.48	15.47	19.43	22.35	25.26
	+4	68	2.95	6.80	34228	5034	1665	9.21	1286	55082	11.14	16.46	20.67	23.95	27.23
	+5	78	3.20	6.96	38953	5600	1785	9.51	1386	63840	11.81	17.46	21.91	25.55	29.20
20	+3	66	2.95	7.73	45696	5963	1986	8.94	1306	72923	14.03	19.06	23.56	28.40	33.12
	+4	76	3.20	7.83	54616	6673	2115	9.21	1406	84235	14.94	20.05	24.77	29.85	34.84
	+5	86	3.45	8.06	57668	7366	2239	9.51	1506	96053	15.47	20.12	26.00	31.36	36.64

DOUBLE JOIST i=62 cm

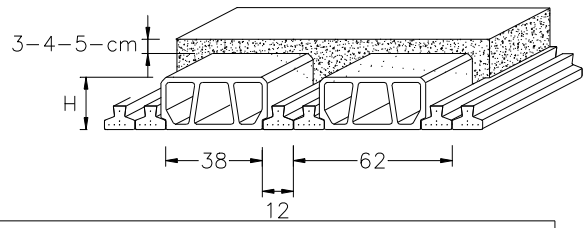

THICKNESS AND WEIGTH FLOOR DATA				TACHNICAL DATA REFERRED TO 1 mt SPAN FLOOR STRIP										
				PARTIAL SECTION				ALL REAGENT SECTION			Me SERVICEABLE POSITIVE MOMENTS kN m			
						MOD. RESIST.					TENDONS JOISTS TYPE			
HOLLOW POT THICKNESS	CONCRETE THICKNESS	CONCRETE QUANTITY	SELF WEIGHT IN SITU	NEUTRAL AXIS	MOMENT OF INERTIA	UPPERSIDE	UNDERSIDE	BARYCENTRIC AXIS DISTANCE	SECTION AREA	BARYCENTRIC MOM. OF INERTIA				
H cm		$\frac{l}{m^2}$	$\frac{kN}{m^2}$	x cm	J cm^4	Ws cm^3	Wi cm^3	Xc cm	Ac cm^2	Jc cm^4	T3	T4	T5	T6	T7
16	+3	75	3.15	7.95	40567	5103	2341	9.46	1312	52874	16.66	23.48	30.07	34.18	38.29
	+4	85	3.40	8.15	47045	5771	2540	9.79	1492	62135	17.73	25.47	32.44	36.48	41.53
	+5	95	3.65	8.37	53873	6434	2736	10.15	1592	72069	18.79	27.43	34.45	39.60	44.47
20	+3	87	3.86	9.17	63026	6875	3037	11.14	1557	83311	22.35	30.06	36.77	43.23	48.59
	+4	97	4.10	9.30	71542	7696	3243	11.44	1657	96058	23.55	31.65	38.80	45.74	51.66
	+5	107	4.34	9.46	80331	8491	3446	11.76	1757	109513	24.74	33.28	40.80	48.25	54.54

SLAB

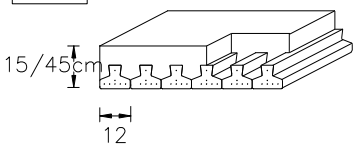

THICKNESS AND WEIGTH FLOOR DATA				TACHNICAL DATA REFERRED TO 1 mt SPAN FLOOR STRIP										
				PARTIAL SECTION				ALL REAGENT SECTION			Me SERVICEABLE POSITIVE MOMENTS kN m			
						MOD. RESIST.					TENDONS JOISTS TYPE			
JOISTS SIZE	SLAB THICKNESS	CONCRETE	SELF WEIGHT IN SITU	NEUTRAL AXIS	MOMENT OF INERTIA	UPPERSIDE	UNDERSIDE	BARYCENTRIC AXIS DISTANCE	SECTION AREA	BARYCENTRIC MOM. OF INERTIA				
cm	H cm	$\frac{l}{m^2}$	$\frac{kN}{m^2}$	x cm	J cm^4	Ws cm^3	Wi cm^3	Xc cm	Ac cm^2	Jc cm^4	T3	T4	T5	T6	T7
9 x 12	15	90	3.75	8,03	33537	4177	3207	8,17	1800	33973	27.47	34.25	37.87	40.69	42.33
	20	140	5.00	10,45	76634	7331	5351	10,85	2300	79570	43.97	55.17	62.44	69.61	74.03
	25	190	6.25	12,64	143436	11369	7754	13,47	2800	153821	60.55	77.03	88.58	99.61	108.67
	30	240	7.50	14,63	237081	16204	10284	16,05	3300	263019	76.50	98.58	115.17	130.08	142.94
	35	290	8.75	16,46	358260	21760	12885	18,61	3800	413435	92.11	119.56	140.83	159.56	175.97
	40	340	10.00	18,17	508515	27981	15532	21,15	4300	611331	107.58	139.25	164.00	186.11	205.67
	45	390	11.25	19,78	688852	34822	18211	23,69	4800	862963	121.97	155.89	181.53	202.65	228.00

		SIMPLE BEARING	BEARING AND RESTRAINED	RESTRAINED AT BOTH ENDS
12	+3	4.00	4.30	4.50
	+4	4.20	4.50	4.80
	+5	4.50	4.80	5.10
16	+3	5.00	5.40	5.70
	+4	5.30	5.70	6.00
	+5	5.60	6.00	6.30
20	+3	6.10	6.50	6.90
	+4	6.30	6.80	7.20
	+5	6.40	7.00	7.40

DESIGN GUIDANCE

In the following schedule are given the spans that can be achieved with the floor joists, in accordance with hint contraints, for normal domestic house leave loads– emphasizing – that only design can give the right one.
The IPCI will be pleased to offer the calculation advice when requested.
In that case:
The maximum positive service moments,are calculated taking into consideration resistant sections made by areas effectively pressed of concrete cast in situ and prestressed joist.
It has also been verified that the breaking factor > 1.5 valuing such method with the stress/strain method according to the limit strain of the stressing wire equal to 1% over decompression.

Having located the external exercise stress Me positive, calculeted according to the usual elastic theory methods,the project calculation is reduced to the solution table finding for whic have been respected at the same conditions Ms > Me.

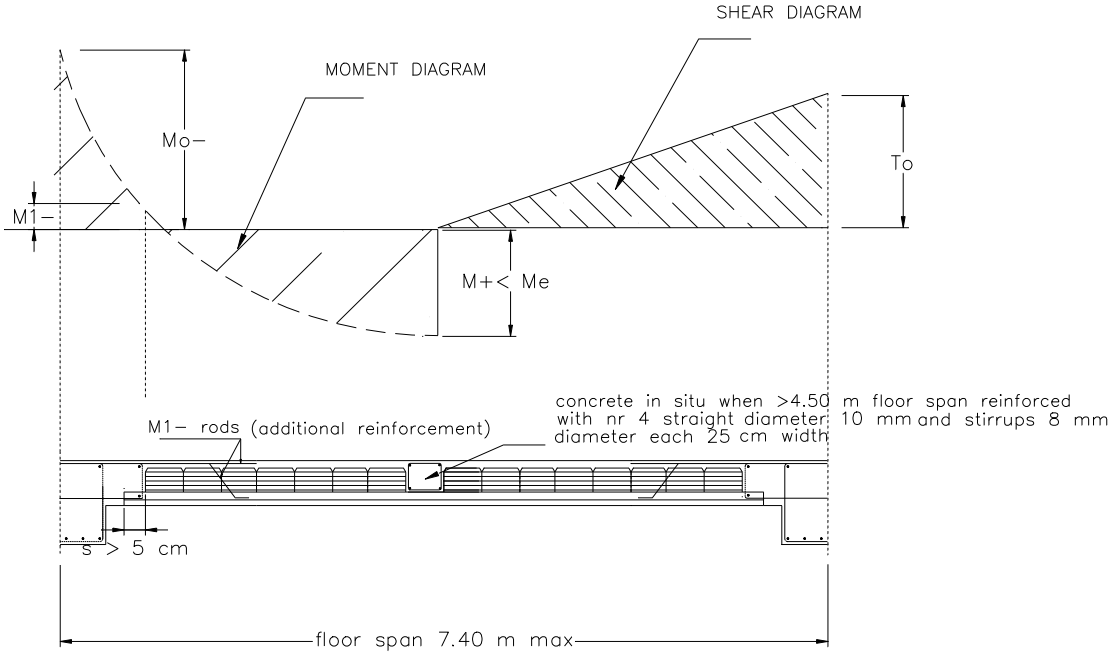

The IPCP light prestressed concrete floors can be used advantageously on every type of bear structures as:

Reiforced concrete
Iron profiles
Masonry

The following detail is for all of that.

CARRING OUT OF A FLOOR HOLE WITH TWO JOISTS SIDE

FLOOR CROSS SECTION

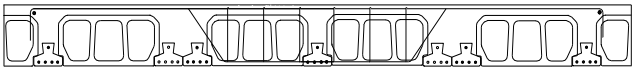

FLOOR PLANT

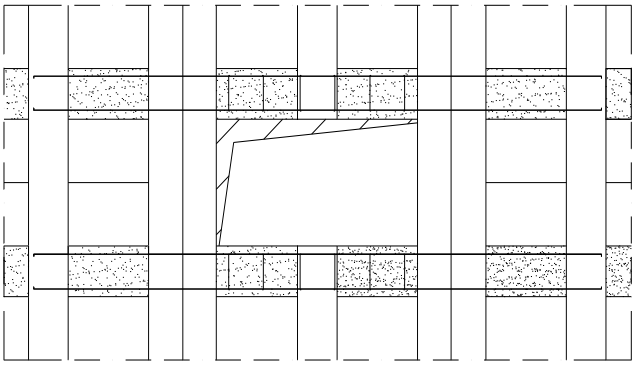

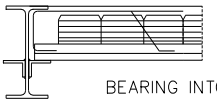

BEARING INTO WEB H–BEAM

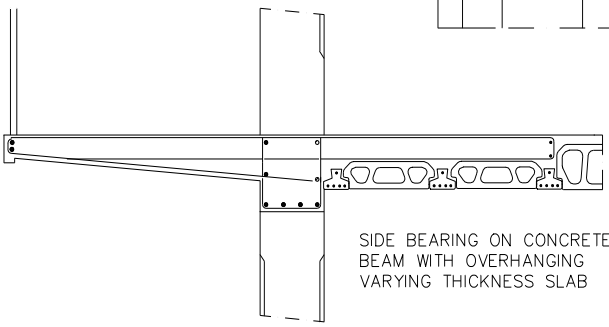

SIDE BEARING ON CONCRETE BEAM WITH OVERHANGING VARYING THICKNESS SLAB

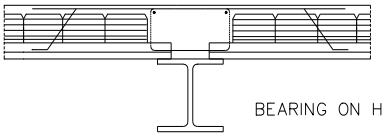

BEARING ON H–BEAM

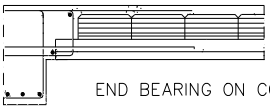

END BEARING ON CONCRETE MAIN BEAM

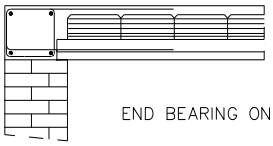

END BEARING ON WALL

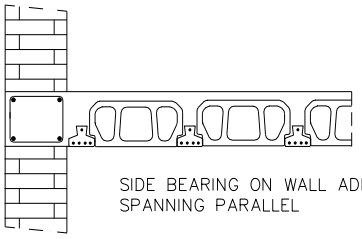

SIDE BEARING ON WALL ADIACENT BAY SPANNING PARALLEL

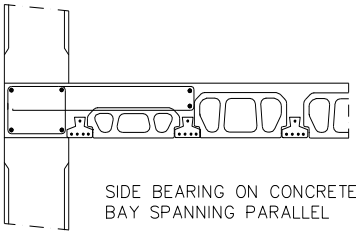

SIDE BEARING ON CONCRETE BEAM BAY SPANNING PARALLEL

APPENDIX C

COMPARISONS FOR SERVICE AND ULTIMATE LOAD

Eurocode design calculation for service and ultimate load

Dead load (DL) (from Trasacco sheet) = 2.95 kPa

(note for 200 mm solid thick slab, Dead load is = 23.6 * 0.2 = 4.72 kPa)

Super-imposed dead load from screed and partititions = 2.5 kPa

Then, total dead load (DL) = 2.95 + 2.5 = 5.45 kPa

Live load (LL) for normal buildings designed for office buildings based on information obtained from EC1 (BS EC1, 2002) LL = 2.0 – 3.0 kPa.

v

Thus the maximum total uniformly distributed service slab load is:

Ws = DL + LL

Ws = 5.45 + 3.0 = 8.45 kPa

The maximum total uniformly distributed ultimate load from EC2 (BS EC2, 2004) is:

TF = 1.35 DL + 1.5 LL

= 1.35 (5.45) + 1.5 (3.0)

= 11.86 kPa

Trasacco technical data calculation

Joist moment = ½ of slab moment

Uniformly linearly distributed load on joist (ω) = 0.5*Ws = Ws/2

T is the service slab maximum moment

$$\frac{\omega l^2}{8} = \frac{T}{2} = \frac{Wsl^2}{16}$$

$$Ws = \frac{8*16.46}{3.8^2} = 9.12$$

The estimated service load is thus 9.12 kPa with the average ultimate load as is 13.2 kPa (i.e. 9.12*1.45, where 1.45 is the approximate ultimate/service load ratio).

APPENDIX D

TYPICAL STRUCTURAL DESIGN DRAWINGS

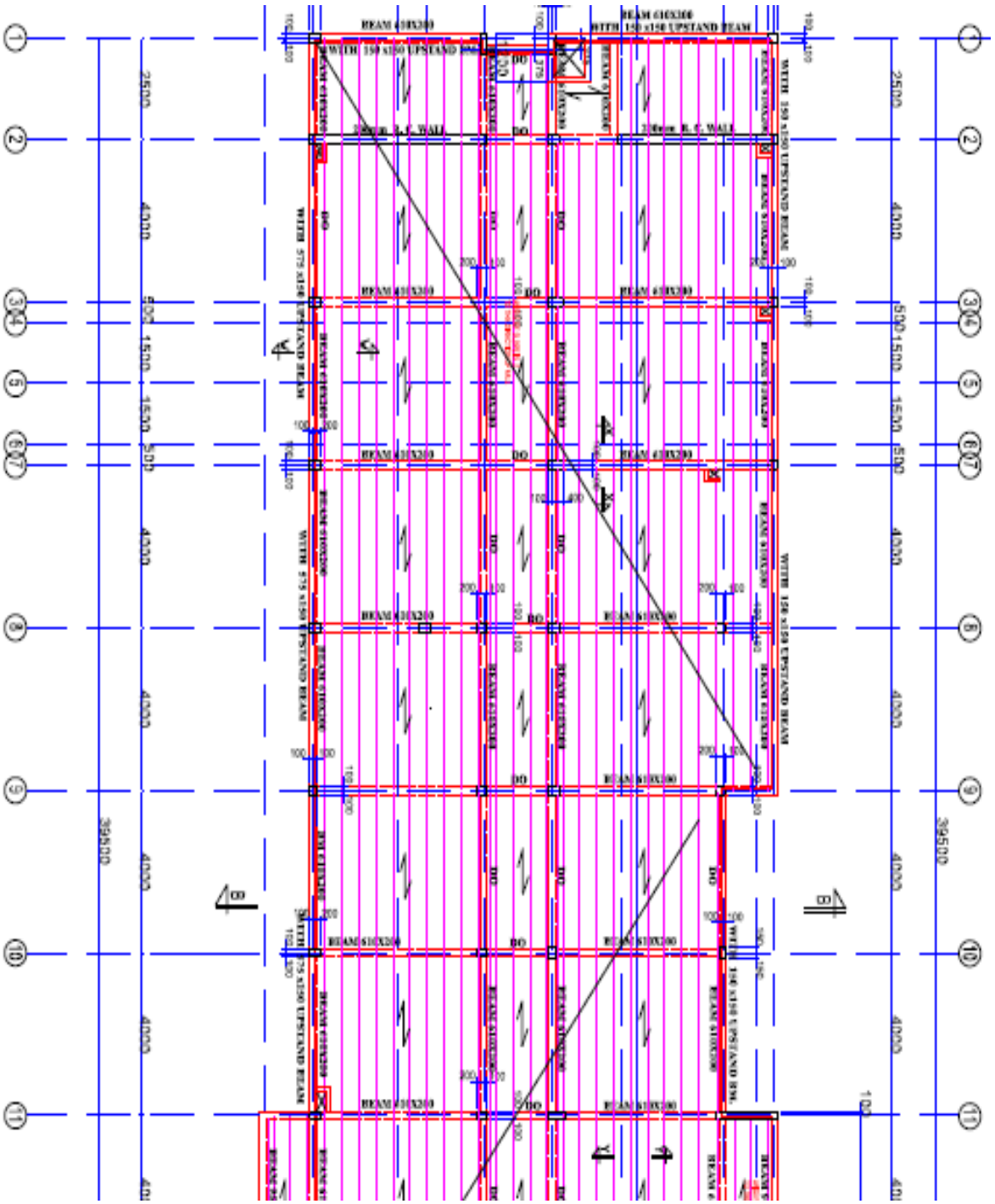

Figure A: Trasacco floor plan

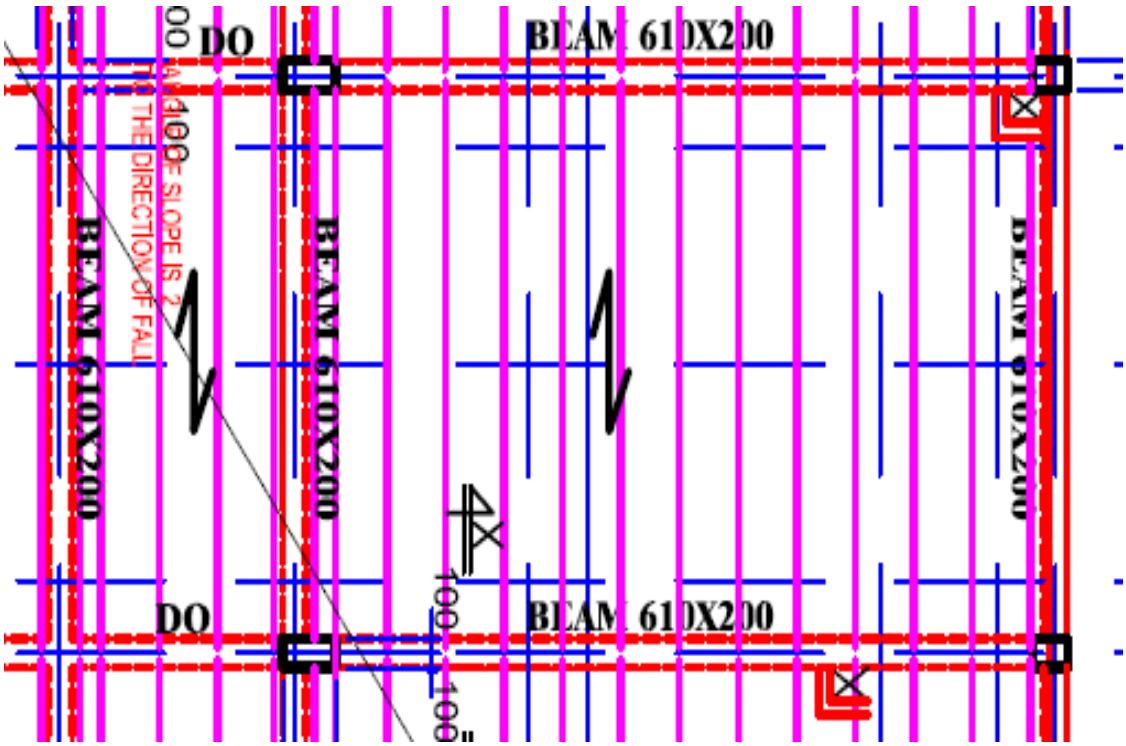

Figure B Section to be modelled